JAERI-M
88-272

ANNUAL REPORT OF THE OSAKA LABORATORY FOR RADIATION CHEMISTRY JAPAN ATOMIC ENERGY RESEARCH INSTITUTE (NO. 20)

April 1, 1986 - March 31, 1987

January 1989

Osaka Laboratory for Radiation Chemistry

日本原子力研究所
Japan Atomic Energy Research Institute

JAERI-Mレポートは，日本原子力研究所が不定期に公刊している研究報告書です。
入手の問合わせは，日本原子力研究所技術情報部情報資料課（〒319-11茨城県那珂郡東海村）あて，お申しこしください。なお，このほかに財団法人原子力弘済会資料センター（〒319-11 茨城県那珂郡東海村日本原子力研究所内）で複写による実費頒布をおこなっております。

JAERI-M reports are issued irregularly.
Inquiries about availability of the reports should be addressed to Information Division Department of Technical Information, Japan Atomic Energy Research Institute, Tokai-mura, Naka-gun, Ibaraki-ken 319-11, Japan.

編集兼発行　日本原子力研究所
印　　刷　㈱高野高速印刷

JAERI-M 88-272

Annual Report of the Osaka Laboratory for Radiation Chemistry Japan Atomic Energy Research Institute (No. 20) April 1, 1986 - March 31, 1987

Osaka Laboratory for Radiation Chemistry
Takasaki Radiation Chemistry Research Establishment
Japan Atomic Energy Research Institute
Neyagawa-shi, Osaka-fu

(Received December 26, 1988)

This report describes research activities of Osaka Laboratory for Radiation Chemistry, JAERI during one year period from April 1, 1986 through March 31, 1987. The latest report, for 1985, is JAERI-M 87-046.

Detailed descriptions of the activities are presented in the following subjects: studies on surface phenomena under electron and ion irradiations; polymerization under the irradiation of electron beams; modification of polymers, degradation, cross-linking, and grafting.

Previous reports in this series are:

Annual Report, JARRP, Vol. 1		1958/1959*
Annual Report, JARRP, Vol. 2		1960
Annual Report, JARRP, Vol. 3		1961
Annual Report, JARRP, Vol. 4		1962
Annual Report, JARRP, Vol. 5		1963
Annual Report, JARRP, Vol. 6		1964
Annual Report, JARRP, Vol. 7		1965
Annual Report, JARRP, Vol. 8		1966
Annual Report, Osaka Lab., No. 1	JAERI 5018	1967
Annual Report, Osaka Lab., No. 2	JAERI 5022	1968
Annual Report, Osaka Lab., No. 3	JAERI 5026	1969
Annual Report, Osaka Lab., No. 4	JAERI 5027	1970
Annual Report, Osaka Lab., No. 5	JAERI 5028	1971
Annual Report, Osaka Lab., No. 6	JAERI 5029	1972

Annual Report, Osaka Lab., No. 7	JAERI 5030	1973
Annual Report, Osaka Lab., No. 8	JAERI-M 6260	1974
Annual Report, Osaka Lab., No. 9	JAERI-M 6702	1975
Annual Report, Osaka Lab., No. 10	JAERI-M 7355	1976
Annual Report, Osaka Lab., No. 11	JAERI-M 7949	1977
Annual Report, Osaka Lab., No. 12	JAERI-M 8569	1978
Annual Report, Osaka Lab., No. 13	JAERI-M 9214	1979
Annual Report, Osaka Lab., No. 14	JAERI-M 9856	1980
Annual Report, Osaka Lab., No. 15	JAERI-M 82-192	1981
Annual Report, Osaka Lab., No. 16	JAERI-M 83-199	1982
Annual Report, Osaka Lab., No. 17	JAERI-M 84-239	1983
Annual Report, Osaka Lab., No. 18	JAERI-M 86-051	1984
Annual Report, Osaka Lab., No. 19	JAERI-M 87-046	1985

* Year of the activities

Keywords: Electron Beam Irradiation, γ-Irradiation, Radiation Induced Reaction, Polymerization, Grafting, Polymer Modification, Radiation Chemistry, Auger Spectrum, Epoxy Resin, Polyethylene Foam, Carbon Film, Fischer-Tropsch Reaction

JAERI－M 88－272

昭和６１年度日本原子力研究所大阪支所年報（No.２０）

１９８６年4月1日～１９８７年3月３１日

日本原子力研究所高崎研究所
大阪支所

（１９８８年１２月２６日受理）

本報告書は，大阪支所において昭和６１年度に行われた研究活動を述べたものである。主な研究題目は，電子及びイオン照射下の界面現象に関する基礎研究，電子線照射による重合反応の研究，ポリマーの改質及び上記の研究と関連して重合反応，高分子の分解及び架橋ならびにグラフト重合に関する基礎的な研究などである。

日本放射線高分子研究協会年報 Vol. 1		1958/1959
日本放射線高分子研究協会年報 Vol. 2		1960
日本放射線高分子研究協会年報 Vol. 3		1961
日本放射線高分子研究協会年報 Vol. 4		1962
日本放射線高分子研究協会年報 Vol. 5		1963
日本放射線高分子研究協会年報 Vol. 6		1964
日本放射線高分子研究協会年報 Vol. 7		1965
日本放射線高分子研究協会年報 Vol. 8		1966
日本原子力研究所大阪支所における放射線化学の基礎研究 No.1	JAERI 5018	1967
日本原子力研究所大阪支所における放射線化学の基礎研究 No.2	JAERI 5022	1968
日本原子力研究所大阪支所における放射線化学の基礎研究 No.3	JAERI 5026	1969
日本原子力研究所大阪支所における放射線化学の基礎研究 No.4	JAERI 5027	1970
日本原子力研究所大阪支所における放射線化学の基礎研究 No.5	JAERI 5028	1971
日本原子力研究所大阪支所における放射線化学の基礎研究 No.6	JAERI 5029	1972
日本原子力研究所大阪支所における放射線化学の基礎研究 No.7	JAERI 5030	1973
Annual Report, Osaka Lab., JAERI, No. 8	JAERI-M 6260	1974
Annual Report, Osaka Lab., JAERI, No. 9	JAERI-M 6702	1975
Annual Report, Osaka Lab., JAERI, No.10	JAERI-M 7355	1976
Annual Report, Osaka Lab., JAERI, No.11	JAERI-M 7949	1977
Annual Report, Osaka Lab., JAERI, No.12	JAERI-M 8569	1978
Annual Report, Osaka Lab., JAERI, No.13	JAERI-M 9214	1979
Annual Report, Osaka Lab., JAERI, No.14	JAERI-M 9856	1980
Annual Report, Osaka Lab., JAERI, No.15	JAERI-M 82-192	1981
Annual Report, Osaka Lab., JAERI, No.16	JAERI-M 83-199	1982
Annual Report, Osaka Lab., JAERI, No.17	JAERI-M 84-239	1983
Annual Report, Osaka Lab., JAERI, No.18	JAERI-M 86-051	1984
Annual Report, Osaka Lab., JAERI, No.19	JAERI-M 87-046	1985

高崎研究所（大阪支所）：〒５７２　大阪府寝屋川市三井南町２５－１

CONTENTS

I. INTRODUCTION

Osaka Laboratory was founded in 1958 as a laboratory of the Japanese Association for Radiation Research on Polymers (JARRP), which was organized and sponsored by some fifty companies interested in radiation chemistry of polymers. The JARRP was merged with Japan Atomic Energy Research Institute (JAERI) on June 1, 1967, and the laboratory has been operated as Osaka Laboratory for Radiation Chemistry, Takasaki Radiation Chemistry Research Establishment, JAERI. The research activities of Osaka Laboratory have been oriented towards the fundamental research on applied radiation chemistry.

The studies on electron- and ion-impact induced adsorption and desorption of gases on solid surfaces are important since they will help understand the phenomena occurred on the first wall surface of present-day and future nuclear fusion reactors.

In an attempt to prepare a model first wall upon which the studies on the adsorption and desorption are to be carried out, studies on carbon deposition from gaseous methane by r.f. glow discharge have been carried out. A diamond like thin film was formed on a quartz or a nickel substrate.

A study to prepare chemically active or inactive surface by electron beam recoil doping on solid surfaces has been continued on a polyimide surface and iron as implanting element. It was found that iron was implanted 100 nm below the surface from the change in the Auger spectrum during the argon ion sputtering, when an amorphous silicon surface was irradiated with 800 keV electrons in the atmosphere of Ar-iron pentacarbonyl gas mixture.

Low energy Kr^+ ion irradiation on Kapton film was carried out and depth profiles of Kr^+ and other elements were obtained by XPS and RBS technique.

The strength and appearance of the film casted from poly(methyl acrylate) emulsion particles were studied as a function of dose, and the results were explained on the basis of changes of surface acidity and elasticity of the particles due to electron beam irradiation.

Grafting of acrylic acid onto polyethylene foam material was

carried out in order to give hydrophilic properties to the foam, and it was found that a foam of excellent hydrophilic properties was obtained by the grafting of low degrees.

Bisphenol A type epoxy oligomers of different molecular weights were cured with electron beams and it was found that the final gel content and the initial rate of reaction depend on molecular weight of the oligomers.

In the study to evaluate the dose absorbed in a thin layer substance when it was exposed to an electron beam, it was elucidated that the backscattering from the backing material is important for precise dosimetry of the film substance. Diffusion length of electrons in p-region of a GaAs solar cell was determined by technique consisted of the current under the electron irradiation.

September 16th, 1988

Dr. Motoyoshi Hatada
Osaka Laboratory for Radiation Chemistry
Japan Atomic Energy Research Institute

II. RECENT RESEARCH ACTIVITIES

1. Preparation of Diamond Thin Films by R.F. Glow Discharge Method

Some carbon containing materials such as graphite and diamond as well as silicon carbide are considered to be promising materials for the first wall in controlled thermonuclear reactors.[1] In order to prepare the carbon materials as specimens for studying on adsorption and desorption of gases on their surface, we have investigated the effects of reaction conditions on deposition of the carbon films from gaseous mixture of methane and hydrogen by the R.F. glow discharge method. It has been reported in the previous annual report[2] that carbon films containing some polycrystalline diamond structure are prepared under the following reaction conditions: methane concentration, 16.7%; total flow rate, 61 ml/min; R.F. power, 100 W; substrate temperature, 180°C; reaction time, 138 min. In an attempt to prepare diamond films with higher crystallinity, further study was carried out on the effects of methane concentration, total flow rate and substrate temperature. The method and techniques used in this report are similar to those employed in our previous study.[2] The properties of the films thus prepared were studied by Auger electron spectroscopy and X-ray diffraction method.

Table 1 shows the reaction conditions that were found to produce carbon thin films on quartz or nickel plates. The films prepared by run nos. 1 ∿ 4 exhibited blackish hue and were electrically conductive. Conversion from electrically conductive to insulating in the deposited film occurred when methane concentration was reduced to 0.8 ∿ 1.0 while the other conditions being kept at those in run no. 4. Thus, run

nos. 6 and 7 gave films that were highly insulating and exhibited yellowish hue or interference fringe.

Figure 1 shows Auger spectra of two typical carbon films prepared by run no. 4(a) and run no. 6(b) on quartz plate. As can be seen, both spectra show carbon KLL Auger peaks with the main peak at 278 eV in addition to oxygen Auger peak at 525 eV. The lineshapes of the carbon spectra for the films a and b agree well with those characteristic of graphite and diamond,[3~5] respectively, indicating that the film a has a graphite-like structure while the film b a diamond-like structure. This assignment is consistent with the electrical properties of the films.

Figure 2 shows X-ray diffraction patterns of the two carbon films prepared by run no. 6(a) and run no. 7(b), both of which proved to have a diamond-like structure by their Auger spectra. Run nos. 6 and 7 differ in the reaction time: 120 min in the condition of run no. 6 and 180 min in that of no. 7. As shown in figure 2(a), the films(a) gives the diffraction peaks at positions corresponding to the interlayer spacings of 1.395, 1.633, 1.916 and 3.137Å. These diffraction peaks are in good agreement with those reported for hexaganol diamond.[6] On the other hand, as shown in figure 2(b), the film gives the diffraction peaks at positions corresponding to the interlayer spacings of 1.107, 1.242, 1.397, 1.441, 1.524, 1.635, 1.92, 1.988, 2.21, 2.286, 2.431, 2.548, 2.733 and 3.14 Å. Among these, the peaks of 1.397, 1.524, 1.635, 1.92 and 3.14Å agree well with those for hexaganol diamond stated above. The peaks of 1.107, 1.242, 1.441, 1.988 and 2.548Å, on the other hand, are in good agreement with those reported for cubic diamond.[7]

The present study shows that diamond thin films with hexaganol or cubic diamond structure can be prepared on quartz or nickel plates from gaseous mixture of methane and hydrogen by R.F. glow discharge method under the following

reaction conditions: methane concentration, 1.0%; total flow rate, 36.5 ml/min; R.F. power, 100 W; substrate temperature, 800°C; reaction time, 120 and 180 min.

(Y. SHIMIZU and S. NAGAI)

1) For example, R. W. Conn, G. L. Kulcinski, H. Avci, and M. EL-Maghrabi, Nucl. Technol., 26, 125(1975).
2) Y. Shimizu and S. Nagai, JAERI-M 87-046, 12-19(1987).
3) T. W. Haas and J. T. Grant, Appl. Phys. Lett., 16, 172(1970).
4) J. T. Grant and T. W. Haas, Surf. Sci., 24, 332(1971).
5) T. W. Haas, J. T. Grant, and G. J. Dooley III, J. Appl. Phys., 43, 1853(1972).
6) ASTM card 26-1082.
7) ASTM card 6-675.

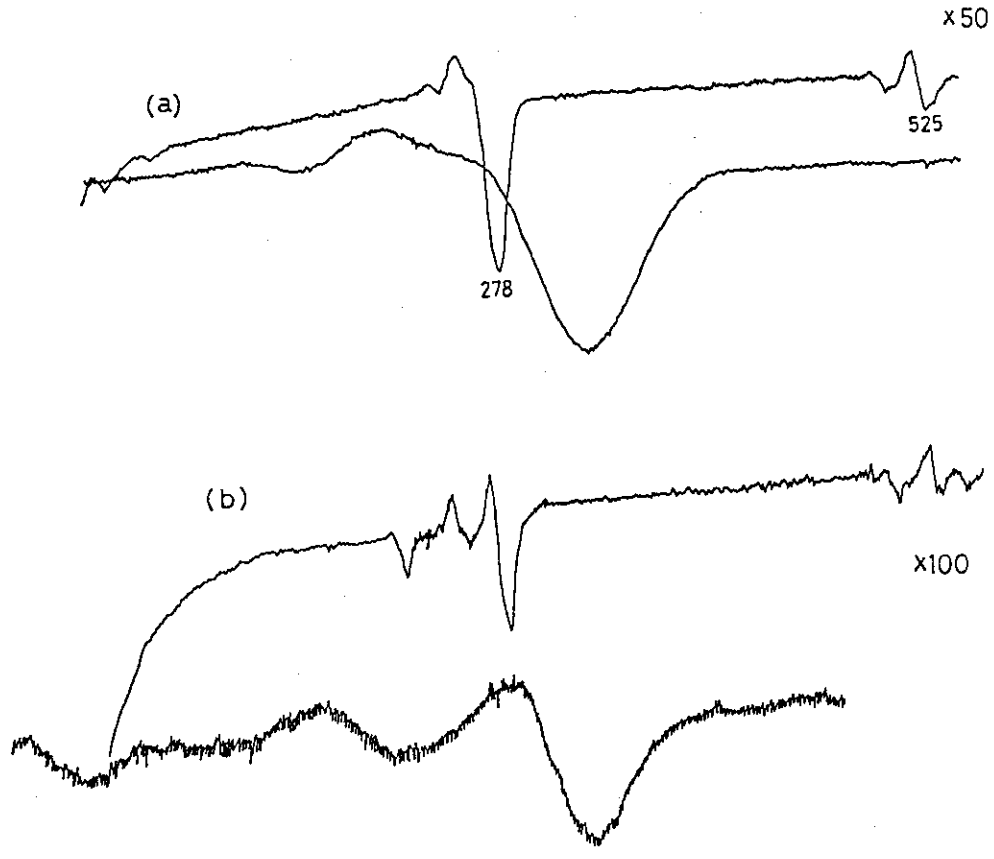

Fig. 1 Auger spectra of the carbon films obtained by run no.4(a) and by run no.6(b). The spectra were recorded at 1.5 keV of electron energy with $5V_{pp}$ of modulation width.

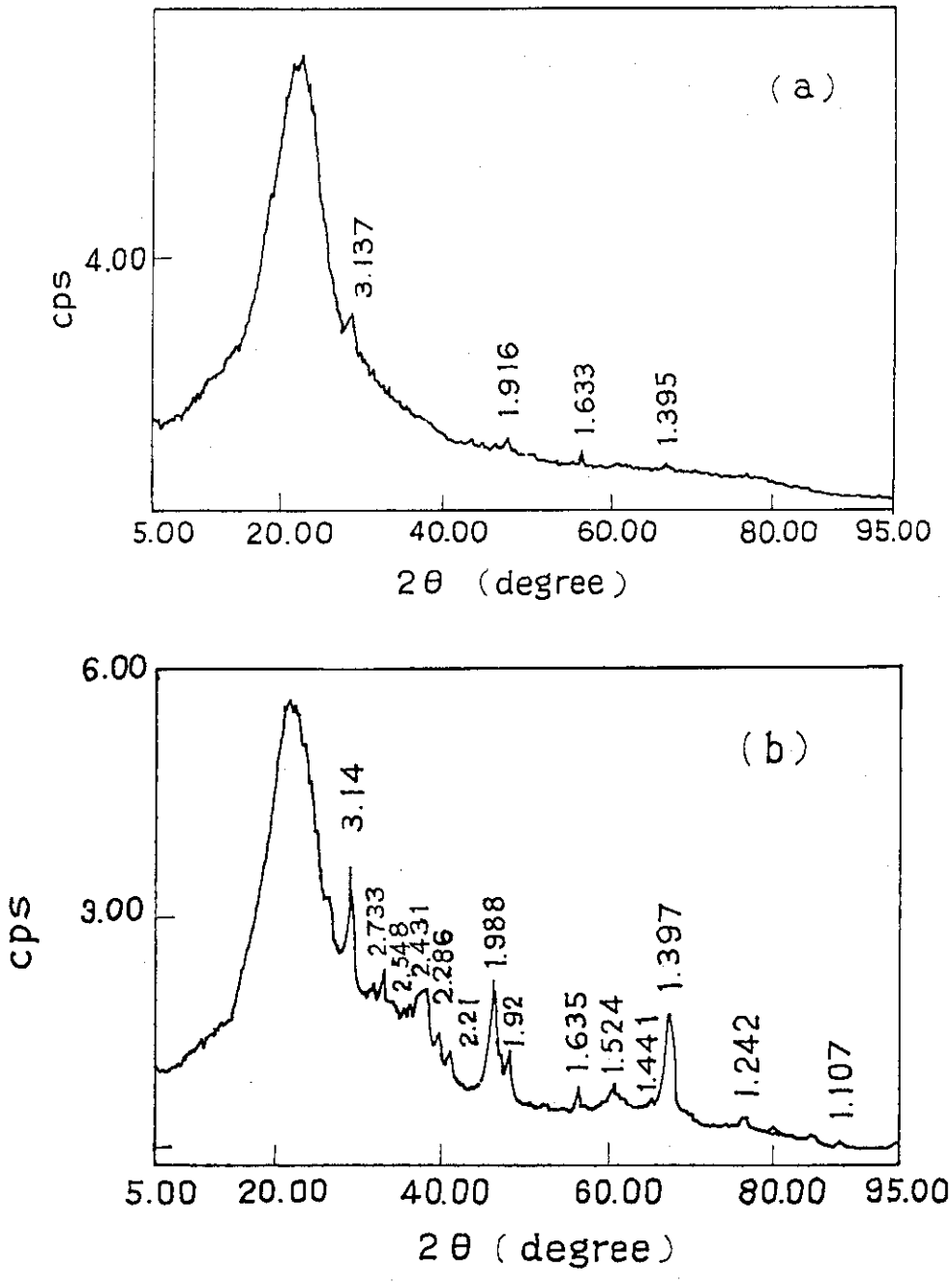

Fig. 2 X-ray diffraction patterns of carbon films obtained by run no.6(a) and by run no.7(b) on quartz plate. The patterns were recorded using Cuk X rays of 60 keV and 200 mA.

2. Catalytic Activity for Fischer-Tropsch Rreaction on a-silicon Doped with Iron

We reported that the Kapton film(Kapton 500H) which had been irradiated with 0.8 MeV electrons in the presence of a gas mixture containing Ar and $Fe(CO)_5$ showed the catalytic activity. In this year, we have carried out a similar experiment on an amorphous silicon(a-silicon) wafer instead of the Kapton film, and the catalytic activity of a-silicon thus prepared has been studied in comparison to that of Kapton film.

A gas mixture of argon gas and a small amount of $Fe(CO)_5$ was irradiated with an electron beam (0.8 MeV, 2 mA) for 14,400 sec, and then the surface of the irradiated a-silicon was dipped in 6 N HCl solution to remove the iron deposited on the surface and then was subjected to the Auger electron spectroscopy (AES) under the argon ion bombardment to obtain depth profile of iron in the a-silicon substrate. The change of the AES with increasing Ar^+ ion bombardment is shown in Fig. 1. The abundance of the element estimated from the AES as a function of depth is shown in Fig. 2 where it is noted that the maximum concentration of iron appears at 100 nm, while the concentrations of carbon and oxygen decreased monotonously as the depth increases. The presence of carbon and oxygen in the surface region may indicate that carbonizataion and oxidation of a-silicon occurred during the electron beam irradiation.

Table 1 shows the results of the catalytic activity test for the Fischer-Tropsch reaction in comparison to the results of the iron doped Kapton film. The activity and selectivity to C_2H_4 (C_2H_6/C_2H_4) are almost the same as those reported for Kapton.

Similar experiments were also carried out using other carrier gas instead of argon and the results are summarized in Table 2. The temperature of the a-silicon surface increased as the atomic number of carrier gas increased. The rate of methane formation was smaller when helium was used as a carrier gas, while it was almost independent of the kind of rare gas for the other rare gases used.

The selectivity to ethylene was almost the same except for xenon

which gave a little higher selectivity. No activity was found when nitrogen was used as carrier gas. The reason for this may be that iron nitride was formed on the a-silicon surface by the electron irradiation and this compound was removed when the irradiated silicon was immersed in 6 NHCl aqueous solution.

The iron doped in the a-silicon was diffused out to the surface by repeated cycles of heating (up to 320°C) and cooling. The iron thus diffused out on the surface was dissolved by HCl aqueous solution and then the amount of iron was determined by colorimetry (at 510 nm) by 1, 10-phenanthroline method. The results are shown in Table 3 where it was noticed that the amount of the iron implanted depends on the kind of rare gas used but differences are not large. The amount of iron implanted increased a little with increasing irradiation time, but increment is smaller than that expected. This is perhaps due to that the iron deposited on the a-silicon surface interferes successive implantation of iron. The rate of methane formation per atom of iron was 1×10^{-3} μmol/(l reactant) and almost the same as that obtained for evaporated iron on the a-silicon.

Fig. 3 shows the catalytic activity as a function of electron accelerating voltage. The activity was first observed for a-silicon implanted at 400 keV and increased with increasing accelerating voltage. The catalytic activity of implanted a-silicon was independent of beam current with which the implantation was carried out. (S. Sugimoto and M. Hatada)

Table 1 Catalytic activity of Fe-implanted amorphus silicon at 304°C

	CH_4	C_2H_4	C_2H_6	C_3H_6
a-Silicon	0.053*	0.016	0.001	0.008
	(1.0)**	0.30	0.02	(0.15)
Polyimide	0.060	0.019	0.003	0.012
(Kapton)	(1.0)	(0.31)	(0.05)	(0.20)

* $\mu mol \cdot l$ reactant$^{-1} \cdot 10$ cm^2 a-silicon$^{-1} \cdot min^{-1}$
** Hydrocarbon ratio

Table 2 Catalytic activity of Fe-implanted amorphus silicon at 304°C

		Yield	Hydrocarbon Content (%)			
Carrier	Temp(°C)	[CH_4*]	CH_4	C_2H_4	C_2H_6	C_3H_6
He	60	0.0092	75.4	11.4	4.1	9.0
Ar	77	0.0129	72.8	17.5	2.2	7.3
Kr	82	0.0124	78.4	13.3	3.1	5.0
Xe	117	0.0116	64.4	25.5	1.1	8.8

* $\mu mol \cdot l$ reactant$^{-1} \cdot 10$ cm^2 a-silicon$^{-1} \cdot min^{-1}$;
Irradiation condition: 800keV, 2mA;
Flow rate of carrier gas: 37 $ml \cdot min^{-1}$;
Reaction condition: $CO:H_2$ = 1 : 4;
Total pressure: 750 Torr;
Temp: 319°C.

Table 3 Amount of iron implanted on the a-silicon surface

Carrier gas	Irrad. time(sec)	Fe(atoms·cm^{-2} a-silicon)*
Ar	14,400	1.9 x 10^{16}
kr	7,200	0.8 x 10^{16}
	14,400	1.0 x 10^{16}
Xe	7,200	1.4 x 10^{16}
	14,400	1.8 x 10^{16}

* determined by colorimetry (1,10-phenanthroline, 510nm)

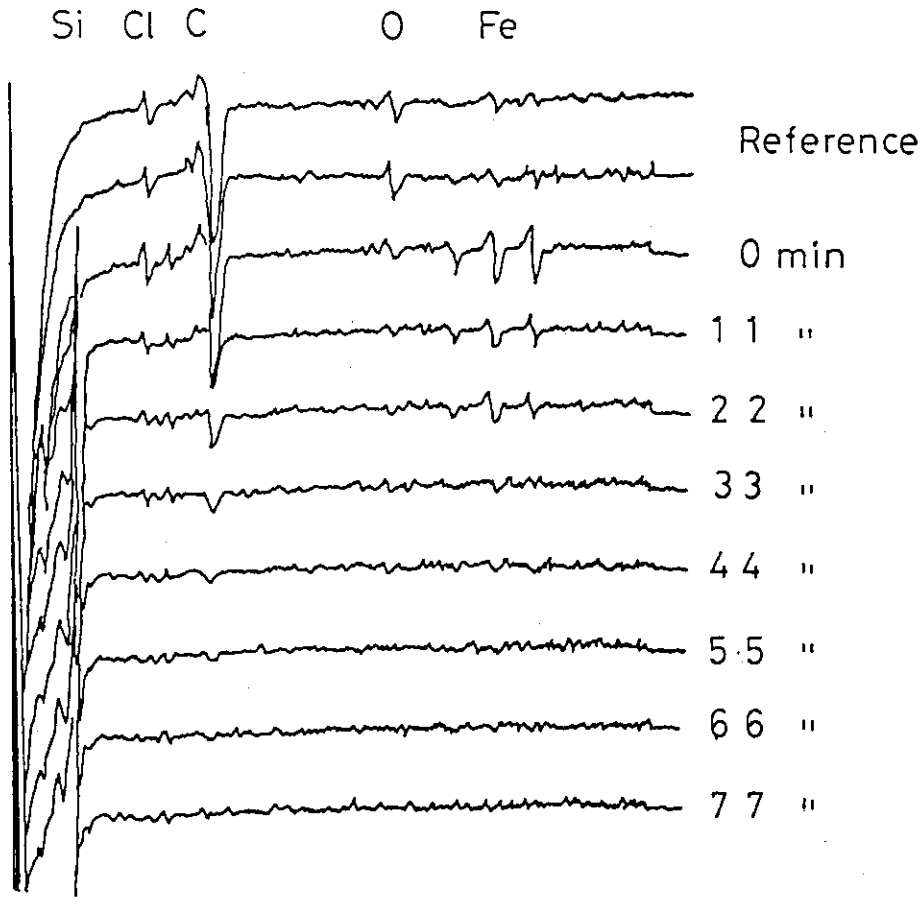

Fig. 1 Auger spectrum during Ar^+ ion sputtering.
(Fe-a-Silicon)

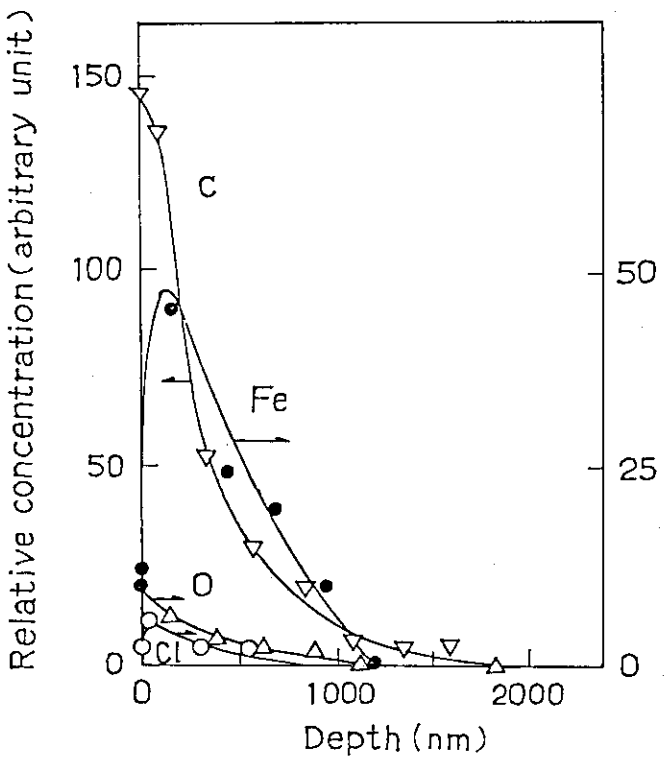

Fig. 2 Depth profile of elements.

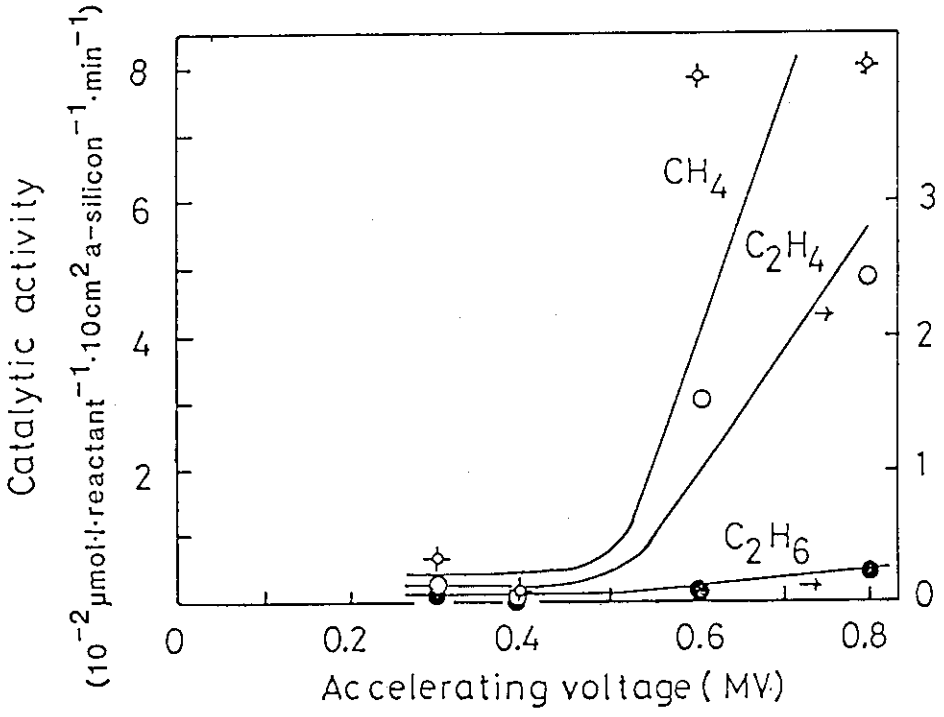

Fig. 3 Relation between catalytic activity and accelerating voltage of electron irradiation.

3. Irradiation of Krypton Ions to Polymer Films

Modification of chemical activities of polymer films by ion irradiation attracts much interest recently. One of the modification methods is the ion-implantation into the polymer films, in which mono- or diatomic ions are considered. In our studies, we intended to irradiate molecular ions composed of several atoms for the surface modification. For this purpose, it is very important to understand how the surface structure changes by ion-irradiation, as well as the behavior of ions implanted into the polymer surface.

A Kapton film was selected as a model polymer because it is thermally stable, and chemically inactive. Krypton was selected as an element to be ionized and accelerated. A preliminary depth-profile study was carried out using X-ray photoelectron spectroscopy(XPS) and Ratherford backscattering spectroscopy(RBS) techniques.

Table 1 shows the theoretical fitting parameters used to describe the RBS spectra by He^{++}(2MeV) of the samples stored at atmospheric environment after ion-irradiation up to 8 months. Depth(nm) in the second column in Table 1 means the layer thickness from the surface, and atomic concentrations at the third column were expressed by two ways, i.e. percent of total atom numbers and normalized numbers to C=22. The amounts of Kr atoms implanted into the Kapton films were estimated from its depth profiles. About 90% of irradiated Kr^{+} dosage was found in the sample stored even up to 8 months.

Since the less amount of N- and O-atoms were found in the nearer region to the surface, it was concluded that the carbonization (graphitization) due to the loss of nitrogen and oxygen atoms at the Kr^{+} irradiated area took place in place of Kr atom-implantation.

The observation of the surface layer of Kr^{+}-irradiated samples by transmission electron microscope revealed that the Kr atoms were kept in the film as bubbles with ca. 15nm diameter up to ca. 300nm depth. (Y. Nakase)

Table 1 Atomic concentration of the samples stored for several periods after Kr-implantation

Stored periods (month)	Depth (nm)	Atomic concentration C(%) (nor)	H(%) (nor)	N(%) (nor)	O(%) (nor)	Kr(%) (nor)
1	0 ～ 30	60 22	35 13	2 0.7	3 1.1	0.5 0.2
	30～160	60 22	31 11	3 1.1	4 1.5	1.8 0.7
	160～200	59 22	29 11	4 1.5	7 2.6	1.4 0.5
	200～230	56 22	27 10	5 2.0	11 4.3	0.7 0.3
	> 230	54 22	26 10	6 2.4	14 5.7	0 0
3	0 ～ 20	60 22	35 13	2 0.7	3 1.1	0.5 0.2
	20～120	60 22	31 11	3 1.1	4 1.5	1.8 0.7
	120～150	59 22	30 11	4 1.5	6 2.2	1.4 0.5
	150～170	56 22	29 11	4 1.6	10 3.9	0.7 0.3
	> 170	54 22	26 10	6 2.4	14 5.7	0 0
5	0 ～ 20	60 22	35 13	2 0.7	3 1.1	0.5 0.2
	20～120	60 22	31 11	3 1.1	4 1.5	1.8 0.7
	120～150	58 22	30 11	4 1.5	6 2.3	1.6 0.6
	150～170	56 22	29 11	4 1.6	10 3.9	0.7 0.3
	> 170	54 22	26 10	6 2.4	14 5.7	0 0
8	0 ～ 20	60 22	35 13	2 0.7	3 1.1	0.5 0.2
	20～120	60 22	31 11	3 1.1	4 1.5	1.8 0.7
	120～150	58 22	30 11	4 1.5	6 2.3	1.6 0.6
	150～170	56 22	29 11	4 1.6	10 3.9	0.7 0.3
	> 170	54 22	27 10	6 2.4	13 5.2	0 0

4. Radiation-Induced Cross-Linking of Poly(Methyl Acrylate)(PMA) Emulsion Particles

The purpose of the present study is to improve the mechanical properties and chemical resistance of the film prepared from polymer emulsion by cross-linking of the polymer emulsion using electron beam irradiation technique.

The PMA emulsion was prepared from methyl acrylate using KPS as catalyst without any emulsifier. The polymer emulsion was irradiated with an electron beam (1.5 MeV, 50 μA) in a sealed glass ampoule for low dose experiments or in an irradiation vessel (capacity, 50ml) with an aluminum window at the top for high dose irradiation experiments. After the irradiation, the gel fraction of the film was measured by the solvent extraction method. The films prepared from the irradiated emulsion were subjected to the tensile strength measurements, observation by electron microscopy, and differential calorimetry, while the emulsion was subjected to dynamical light scattering analysis and electric conductivity titration to measure particle size and surface charge.

The gel percent, water absorption, tensile strength and elongation at the break are plotted as a function of dose in Fig. 1 with the appearance of the film as visually inspected. Smooth surface was observed by 20,000 - 30,000 magnification in the region where no cracks appeared, but rough surface with particle grain pattern was observed near the cracks, indicating that the particles were hard enough to retain their shapes in the film forming process.

The tensile strength increased with dose, reached a maximum value at 60 Mrad and then decreased when the irradiation continued further. The elongation at the break decreased with increasing dose. Two peaks appeared in the DSC curve of unirradiated film as shown in Fig. 2a. The glass transition temperature, Tg_1 increased from 13°C to 19°C by the irradiation of 250 Mrad as shown in Fig. 2b. The Tg_2 appeared below 0°C also increased with dose, but to what process this transition corresponds is not known at present.

The average radius of the emulsion particles obtained by the dynamical light scattering measurement is plotted as a function of dose in Fig. 3, where it is evident that the radius increased with dose.

The surface charge of the irradiated polymer emulsion obtained by the electric conductivity method is plotted as a function of dose in Fig. 4. The amount of surface charge caused by carboxylic acid increased with dose, indicating that the hydrolysis of acrylic ester occurs during the electron irradiation. (T. Yamamoto, M. Nishii, and Y. Doi)

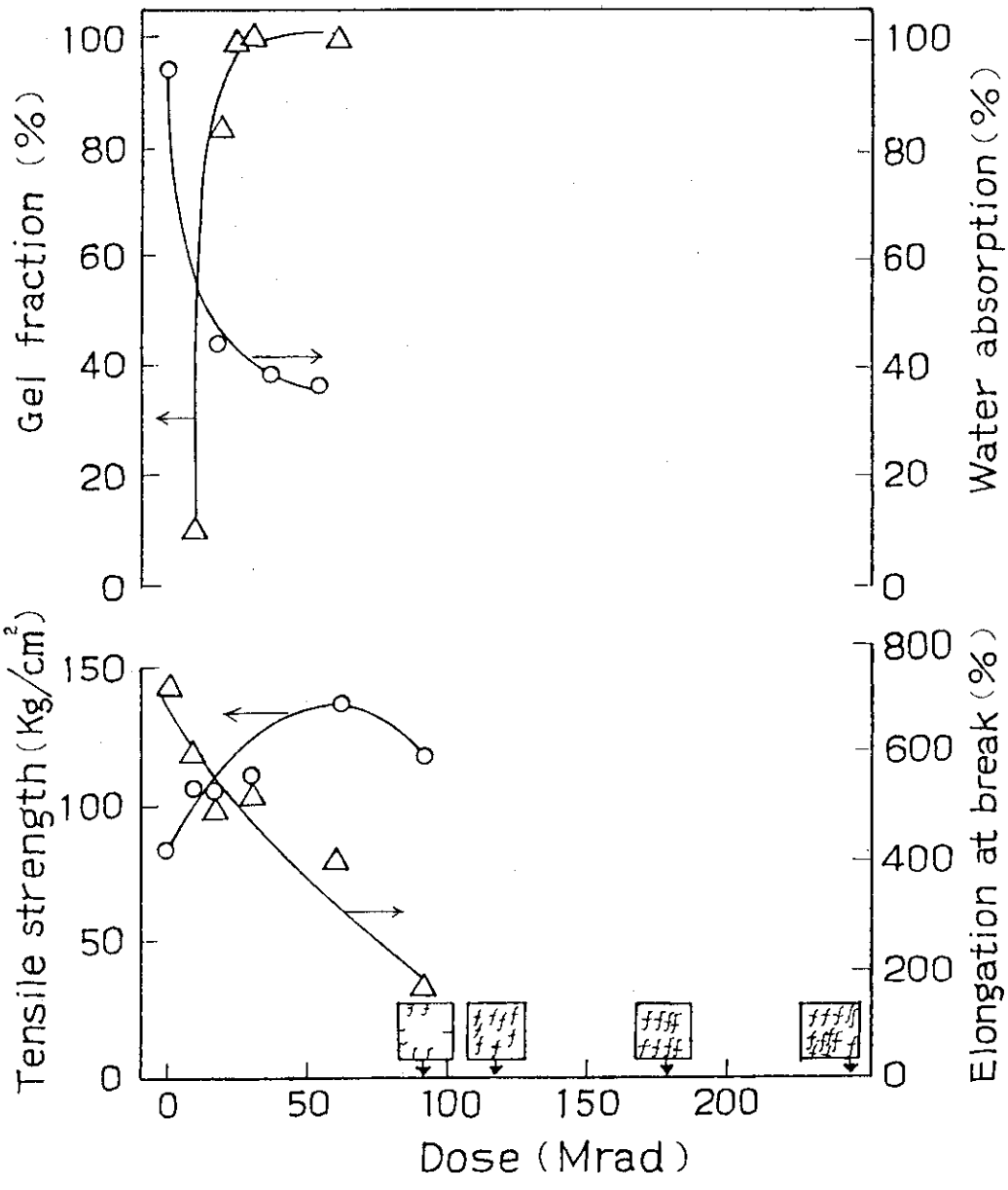

Fig. 1 Properties of films prepared from irradiated PMA emulsion.

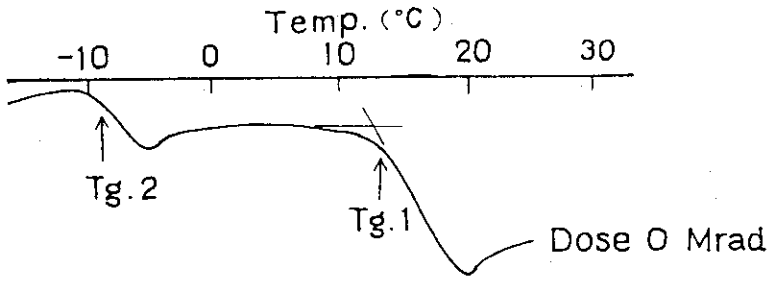

Fig. 2a DSC curve of the film prepared from unirradiated emulsion.

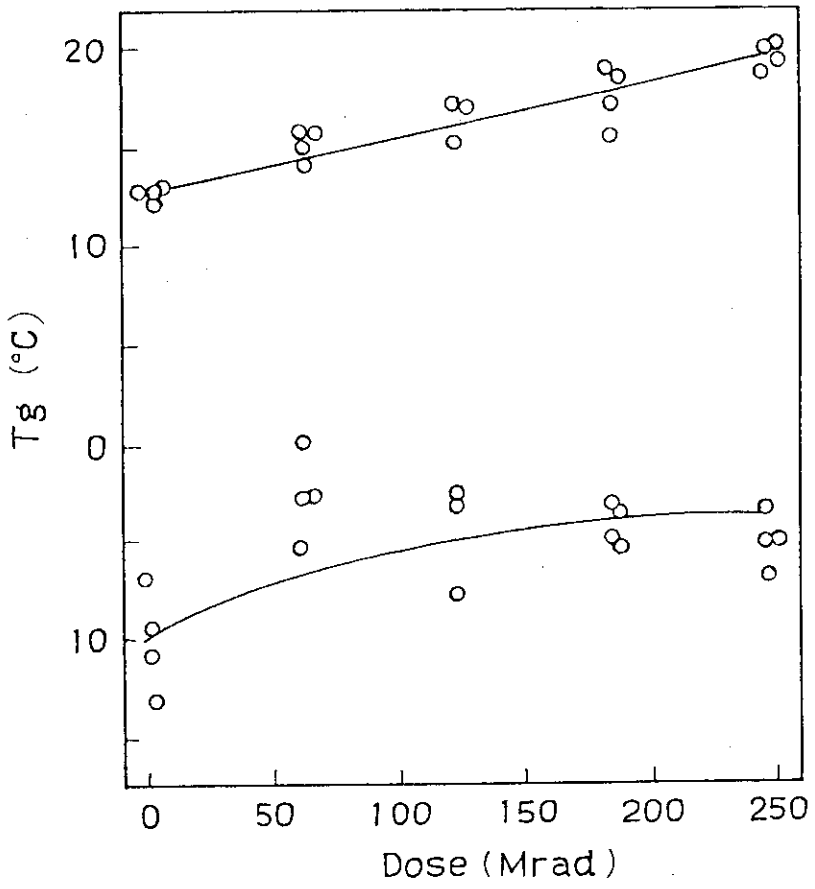

Fig. 2b Fig. glass transition temperature of the polymer prepared from the irradiated PMA emulsion.

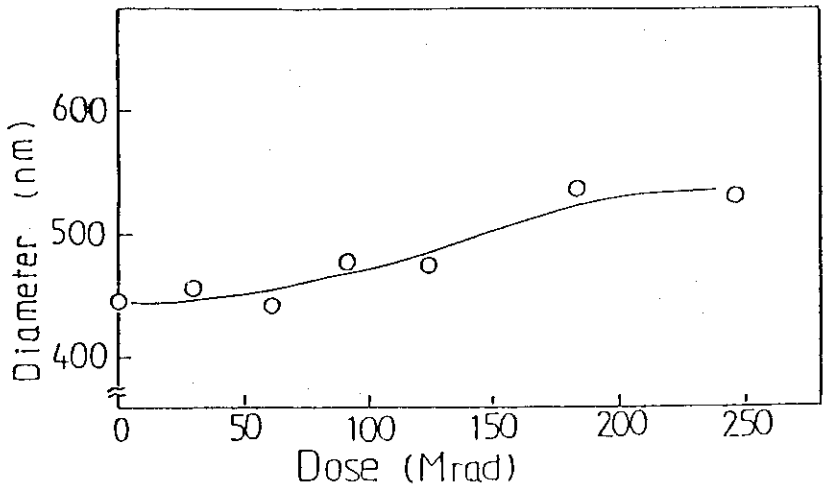

Fig. 3 Particle diameter of the irradiated PMA emulsion as a function of dose.

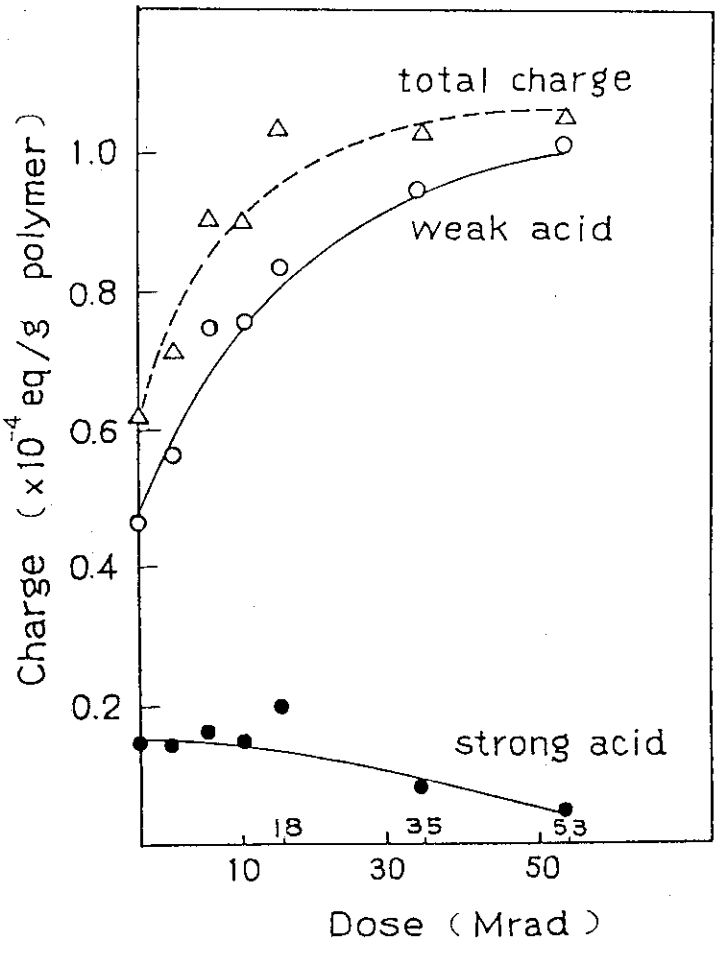

Fig. 4 Surface charge of the irradiated PMA emusion.

5. Electron Beam Curing of Bisphenol A Epoxy Oligomers of Different Molecular Weights

Curing of epoxy oligomers has been carried out by electron beam irradiation and the effects of molecular weights have been studied on the curing behavior. Six oligomers of bisphenol A diglycidyl ether, liquid and solid states, of different molecular weights used in the study are shown in Table 1. An oligomer sample containing 5 x 10^{-2} mol/kg, based on oligomer weight, of bis 4-(diphenylsulfonio)phenyl sulfide-bis-hexafluorophosphate as initiator was dissolved in THF and cast to a viscous liquid film on a slide glass plate. The plates were put in a draft and then in a vacuum oven at 30°C to remove THF. The oligomer films(11 mg/cm^2) were irradiated in air with electron beams of 1.5 MeV from a Van de Graaff accelerator. The irradiated films were subjected to extraction with acetone and the gel contents were gravimetrically determined. The gelatin curves at 0.075 Mrad/s are shown in Fig. 1 and Fig. 2 for two liquid oligomers and for four solid oligomers, respectively.

In the irradiation of liquid oligomers a slightly higher initial gelation rate is obtained for the low molecular weight oligomer, Epikote 828. In each oligomer a levelling-off gel content of 95% was attained at a dose of 18 Mrad. The irradiations of four solid oligomers gave different features from the liquid oligomers. The values of final levelling-off gel contents decreases with increasing molecular weight of the original oligomer. The oligomer of the highest molecular weight , Epikote 1010, retained 37% of soluble part even after the irradiation of a large amount of dose. Initial gelation rate decreases with increasing molecular weight of the original solid oligomer except the irradiation of Epikote 1010.

Decrease in initial gelation rate with increasing molecular weight of the original oligomer in the liquid or solid state can be considered to be due to lowering of epoxide group content in the higher molecular weight oligomer. The initial gelation rate was higher in the solid oligomer than in the liquid oligomer.

The changes in the functional groups of epoxy oligomers, epoxide, ether and hydoxyl groups with the electron beam curing have been studied by infrared spectrometry. The results are shown in Fig. 3, Fig. 4 and Fig. 5. For all oligomers, the intensity of epoxide band decreased monotonousely, whereas those of hydroxyl and ether bands increased with irradiation dose. Absorbance ratios of each functional group at 18 Mrad irradiation are given in Table 2, together with those of the unirradiated oligomers. Unreacted epoxide groups still remained in all oligomers, although the gel content had almost reached its maximum.

The levelling-off gel contents in the oligomers of different molecular weight are shown in Table 3. For comparison, the datas obtained with ultraviolet curing are also included in the table.

The results obtained for the oligomers containing 5×10^{-2} mol /kg of initiator with ultraviolet irradiation are compared with those obtained with the electron beam irradiation. In both cases the final levelling-off gel contents decrease with increasing molecular weight of the original oligomer, and lower levelling-off gel contents comapared to those obtained by the irradiation with ultraviolet beams were obtained with electron beam irradiation for all oligomers studied. This might be due to the occurrence of main chain scissions with the irradiation of high energy electron beam. (T. Okada, J. Takezaki, and T. Asano)

Table 1 Molecular weights of epoxy oligomers.

Grade	n	MW	MW_N*	MW_W*	MW_W/MW_N*
Epikote 828	0.1	380	324	368	1.1
Epikote 834	0.5	470	501	779	1.6
Epikote 1001	2	900	988	2060	2.1
Epikote 1004	4	1600	2060	4940	2.4
Epikote 1007	9	2900	3560	10200	2.9
Epikote 1010	18	5500	6850	53200	7.8

* Molecular weights determined by GPC with polystyrene standards.

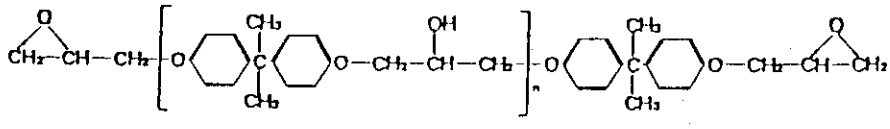

Table 2
Absorbance ratios of functional groups in epoxy oligomers before and after EB-irradiation

Grade	MW	Absorbance ratio, $I = D/D_{830}$					
		Hydroxyl 3500 cm^{-1}		Ether 1108 cm^{-1}		Epoxide 916 cm^{-1}	
		I_0	I_D	I_0	I_D	I_0	I_D
Epikote 828	380	0.036	0.16	0.076	0.32	0.32	0.14
Epikote 834	470	0.10	0.25	0.13	0.40	0.22	0.064
Epikote 1001	900	0.21	0.32	0.21	0.35	0.11	0.028
Epikote 1004	1600	0.25	0.30	0.25	0.38	0.075	0.024
Epikote 1007	2900	0.27	0.29	0.25	0.32	0.059	0.018
Epikote 1010	5500	0.28	0.28	0.25	0.30	0.046	0.020

I_0 = Absorbance ratio of original oligomer,
I_D = Absorbance ratio at 18 Mrad of EB-irradiation.

Table 3
Levelling-off gel contents for UV- and EB-curing

Grade	Irradiation condition	
	UV	EB
	Levelling-off gel content, %	
Epikote 828	99	96
Epikote 834	98	96
Epikote 1001	96	93
Epikote 1004	88	83
Epikote 1007	81	69
Epikote 1010	72	63

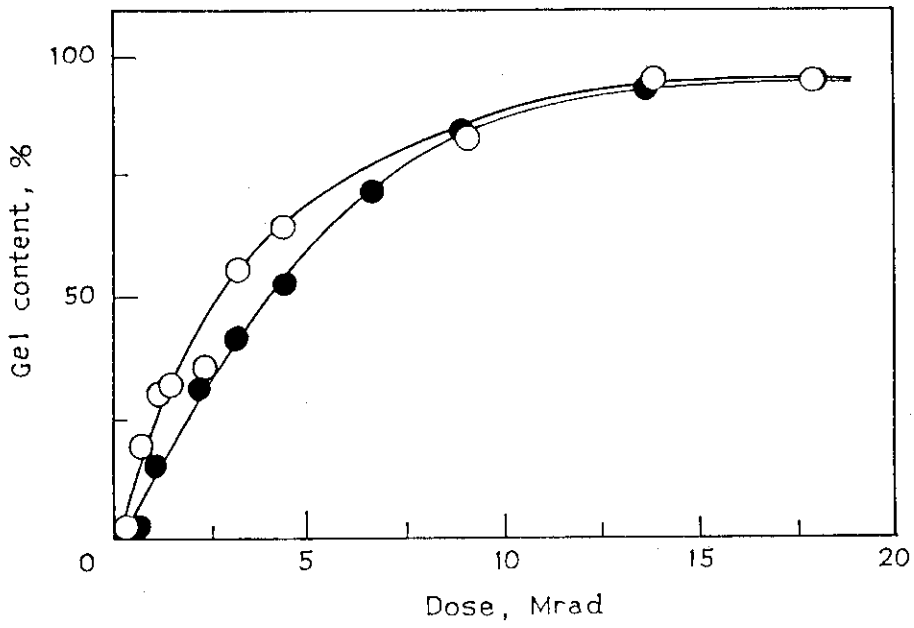

Fig. 1 Gelation curves of liquid epoxy oligomer of different molecular weights. (○)Epikote 828 (n=0.1, MW 380), (●)Epikote 834(n=0.5, MW 470).

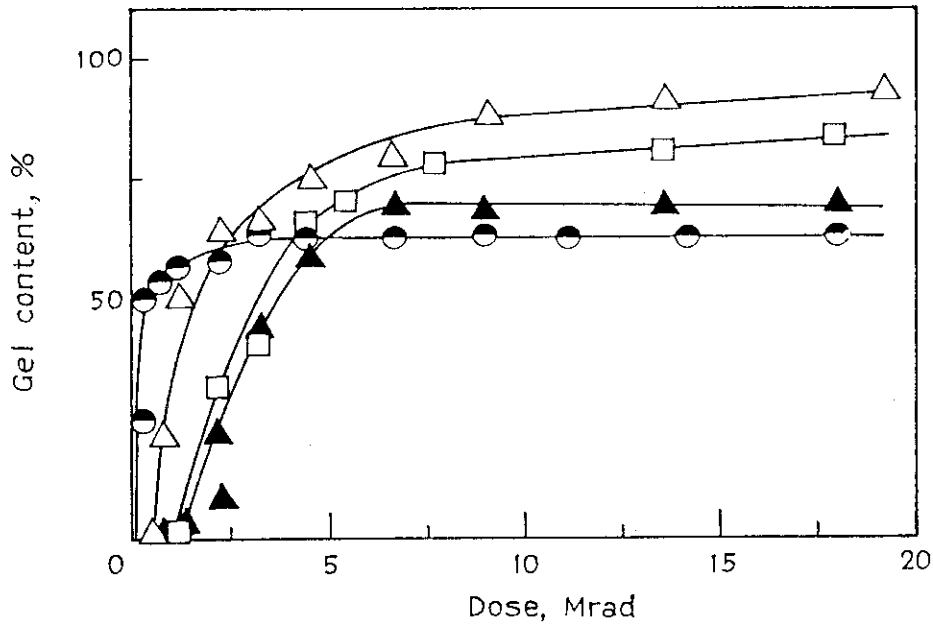

Fig. 2 Gelation curves of solid epoxy oligomers of different molecular weights. (△)Epikote 1001(n=2, MW 900), (□)Epikote 1004(n=4, MW 1600), (▲)Epikote 1007(n=9, MW 2900), (◓)Epikote 1010(n=18, MW 5500).

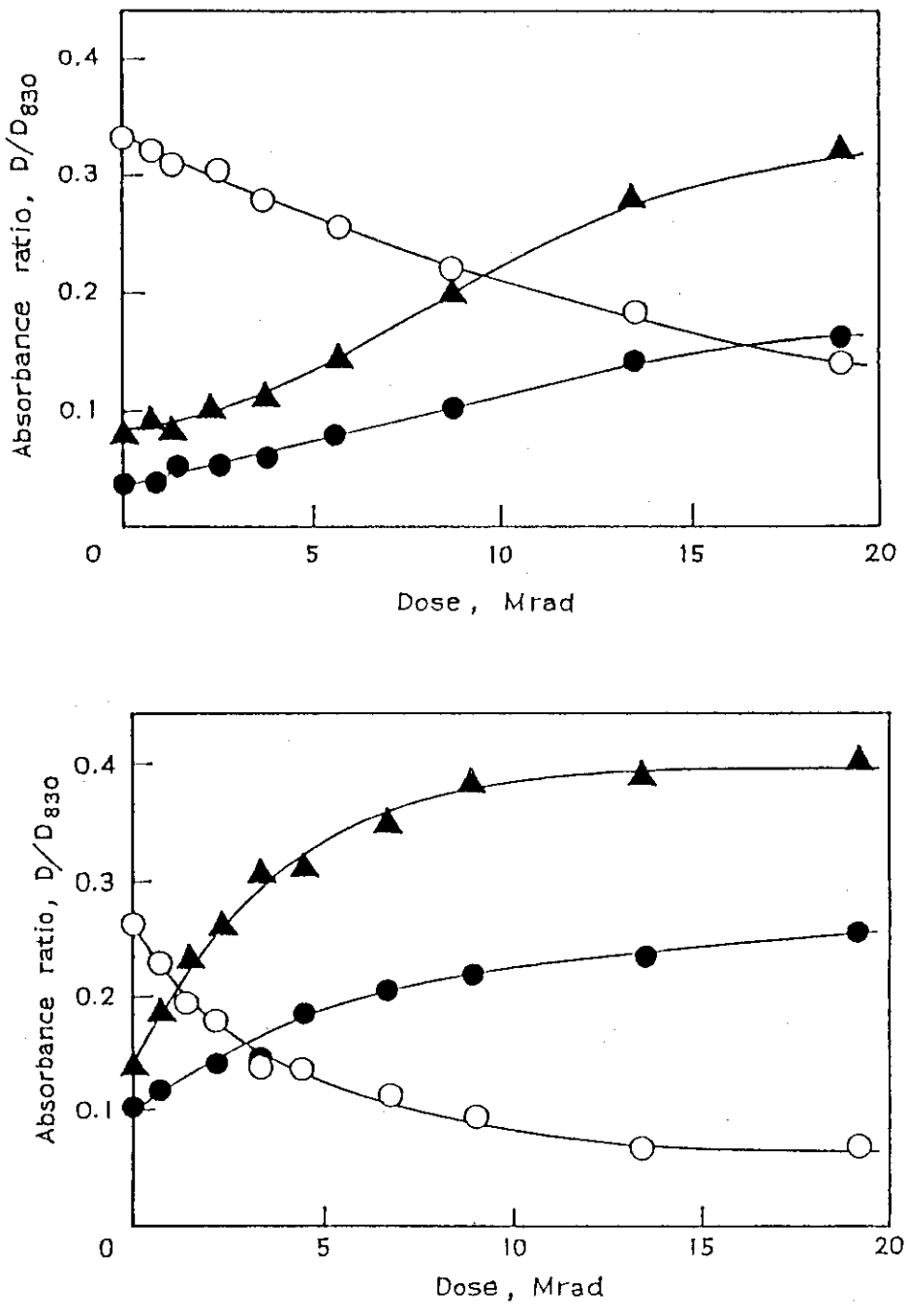

Fig. 3 Changes in functional groups of liquid epoxy oligomers with electron beam irradiation. (○)epoxide, 916 cm^{-1}, (●)hydroxyl, 3500 cm^{-1}, (▲)ether, 1108 cm^{-1}. Upper diagram: Epikote 834, lower diagram: Epikote 834.

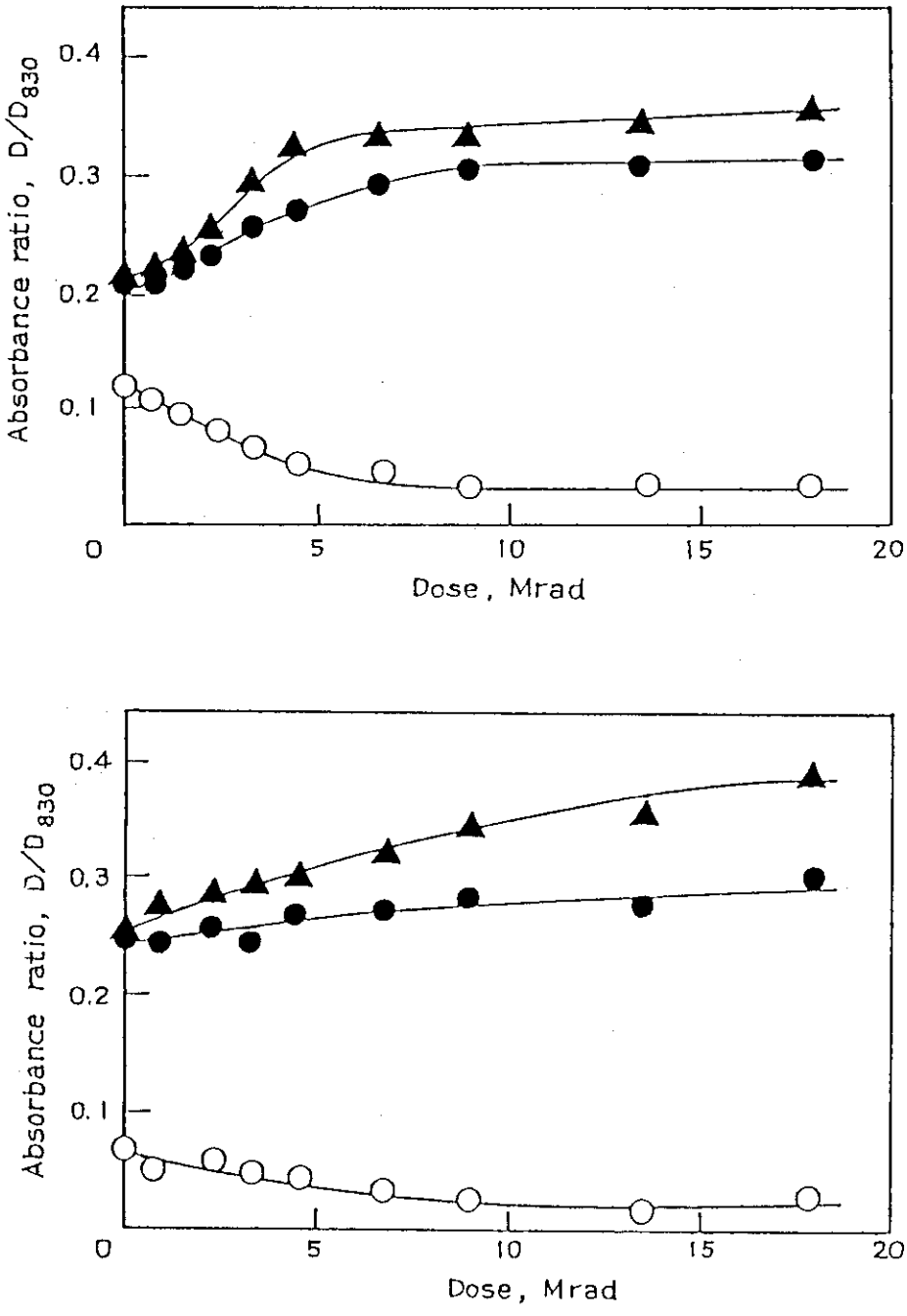

Fig. 4 changes in functional groups of solid epoxy oligomers with electron beam irradiation(1). Upper diagram: Epikote 1001, lower diagram: 1004, symbols are the same as in Fig. 3.

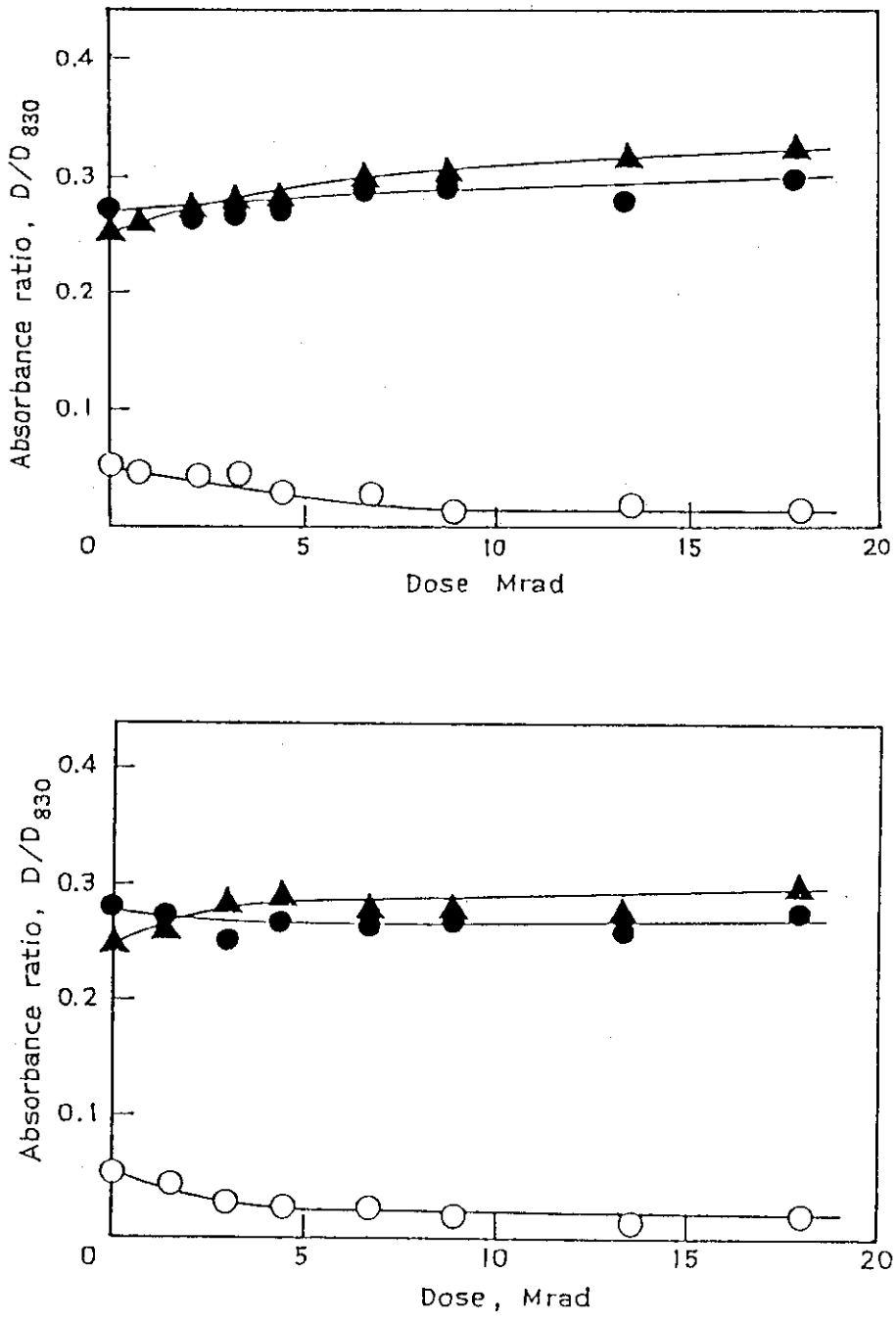

Fig. 5 Changes in functional groups of solid epoxy oligomers with electron beam irradiation(2). Upper diagram: epikote 1007, lower diagram: Epikote 1010, symbols are the same as in Fig. 3.

6. Preparation of Anti-Static Polyethylene Foam of Open Cell Type by Radiation Grafting of Acrylic Acid

The present study has been carried out on the radiation-induced grafting of acrylic acid onto polyethylene foam of open cell type in an attempt to modify the foam to give hydrophilic property. Brief descriptions are made on the grafting behavior of acrylic acid by preirradiation method and also on the hydrophilic properties of the grafted foam thus obtained. The open cell type polyethylene foam was supplied by Sanwa Kako Co. (type LC-300 #2, thickness, 0.5 cm; apparent density, 0.0288 g/cm^3; average radius of cell, 1 mm).
Acrylic acid (AA) of extra-pure grade containing 200 - 500 ppm hydroquinone monomethyl ether as stabilizer was purchased from Nakarai Chemicals Co. and was used as received. Mohr's salt used as inhibitor was also supplied by Nakarai Chemicals Co., and was of guaranteed reagent grade. The foam cut to an appropriate size was sealed in a polyethylene bag in nitrogen atmosphere, and then irradiated with an electron beam (1.5 MeV and 50 μA) from a Van de Graaff accelerator, at dose rate of 1.75 x 10^5 rad/sec.

After the irradiation the foam was transferred to a reaction vessel containing the monomer solution without exposing it to air and was impregnated with monomer solution by repeated cycles of mechanical compression and expansion in nitrogen atmosphere. The reaction vessel was warmed for grafting in a water bath kept at 35°C for the desired reaction time. After the grafting procedure, the foam was taken out from the reaction vessel, washed by running water and further dipped in 50°C water for more than 6 hrs to remove the homoplymer. After the removal of the homopolymer, the grafted foam was dried in a vacuum oven for a constant weight and the graft percent was calculated from the weight increase after the grafting procedure.

In Fig. 1, the graft percent is plotted as a function of reac-

tion time for the monomer solutions (AA : H_2O = 50 : 50 and 95 : 5 by vol.) containing different amounts of Mohr's salt and acrylic acid at 35 °C and at pre-irradiation dose of 5Mrad. At any concentrations of Mohr's salt and acrylic acid, the graft percent increased rapidly at the early stage of the reaction and reached the level-off values which are referred as the final graft percent(FGP). As shown in the figure, the initial increase of conversion is too high to allow a precise determination of the initial rate of grafting but it is still apparent enough to confirm that the higher the initial rate of graftings, the higher the FGP obtained. The FGP depends on the concentrations of both Mohr's salt and acrylic acid in the monomer solution; higher FGP was obtained by lowering the Mohr's salt concentration, and also by increasing the concentration of acrylic acid if the Mohr's salt concentrations are the same. It is noted that the graft percent reached almost the level-off value of 30% in 15 minutes at acrylic acid concentration even as low as 5%.

The FGP is plotted as a function of Mohr's salt concentration in Fig. 2, where it is evident that the graft percent depends on the concentration of Mohr's salt at high monomer concentration: at monomer concentration of 50%, the FGP decreased from 100% to 60% by increasing concentration of Mohr's salt from 4×10^{-3} mol/l to 8×10^{-3} mol/l. But further increase of Mohr's salt concentration resulted a little decrease of FGP. It is also clear from the figure that as the monomer concentration decreases, the effect of Mohr's salt concentration on FGP becomes smaller and at the 5% monomer concentration, only 5% decrease of FGP was observed with the increase of Mohr's salt concentration by an order of magnitude from 4×10^{-4} mol/l.

Figure 3 shows the effect of monomer concentration on the FGP. At concentration of Mohr's salt of 10^{-4} mol/l, the FGP increases linearly with increasing monomer concentration in the range between 5 and 50%, while at 10^{-3} mol/l Mohr's salt concentration, the FGP does not increase linearly but the slope becomes less steep as the monomer concentration increases. The reason for this may be that Mohr's salt prohibits some of grafting of acrylic acid.

In Fig. 4, the FGP is plotted as a function of pre-irradiation

dose. The FGP increased with the increasing dose up to 5 Mrad, but the increment of the FGP with increasing dose became smaller above 5 Mrad. The radicals are built up in the crystalline region of polyethylene during the irradiation. These radicals migrate out from the place where they were originally trapped to the surface of the crystallites and then undergo the grafting reaction with monomers competing with recombination reaction between radicals. Thus, the higher the dose, the higher the concentration of the released radicals on the crystallite surface, resulting in inefficient consumption of radicals for the grafting. This may account for the observed small increment of FGP with dose above 5 Mrad.

The original polyethylene foam cannot be dyed at all, but it turns to be dyeable with cationic dyes when carboxylic groups are introduced to the polyethylene chains. Homogeneous but poor dyeability was obtained by 2% grafting when the grafted foam was dyed with Sevron Brilliant Red B by the method mentioned in a former report[3], but for satisfactory deep dyeability, grafting of more than 20% graft percent was necessary.

The half life of decay of the electric potential built-up on the foam surface was measured by a static honest meter (Shishido Electric Measuring Instruments Co.). High electric field (1kV) was applied across the foam to charge up the surface up to a constant potential and then the electric field was removed to measure the decay of the potential of the surface. The time required for the decay to the half value of the initial voltage was used for an evaluation of the antistatic property.

The results are shown in Fig. 5 where the half-life time is plotted as a function of graft percent at 60% relative humidity. The 50% grafting decreased the half-life of 8000 sec of the original foam to only 1 sec, which was short enough the grafted foam to be used as antistatic foam. The half-life of the grafted foam converted to sodium salt was even shorter than 1 sec which was below the range of the measurement.

The other measurement to evaluate antistatic properties by surface resistivity was carried out using a Fluke 8060A digital multimeter.

The results are shown in Table 1. The surface resistivity of 10^{16} ohm of the original foam decreased to 10^{11} ohm by the grafting of ca. 50% graft, which is sufficient to prevent the surface from charge build-up. The resistivity was further decreased by converting the grafted foam to sodium salt: e.g., the resistivities of 10^{6} ohm and 10^{5} ohm were obtained for the grafted foam of 50% and 100% graft, respectively.

The antistatic properties given by the grafting come from the ionic conduction in the presence of water, and therefore, the antistatic properties may be somewhat poorer in the dried atmosphere.

(K. Kaji, I. Yoshizawa, C. Kohara, K. Komai, and M. Hatada)

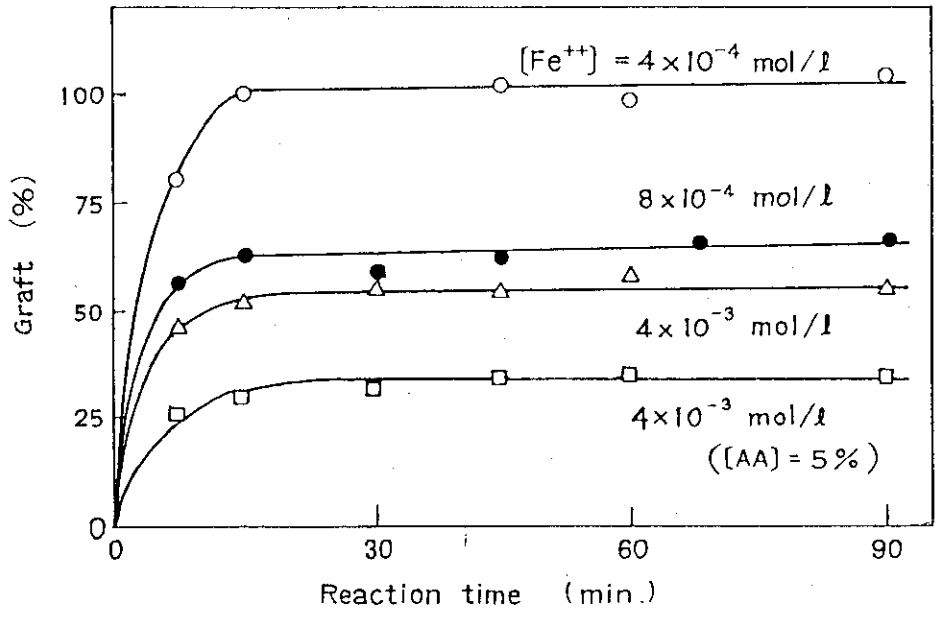

Fig. 1 Grafting of acrylic acid onto polyethylene foam at different concentrations of Mohr's salt; (o) 4 X 10^{-4} mol/l, (△) 8 X 10^{-4} mole/l, (▲) 4 X 10^{-4} mol/l; Preirradiation dose: 5Mrad; Concentration of AA: 50% by volume; Reaction Temperature: 35°C; The time conversion curve obtained for the monomer solution containing 5% AA and 4 X 10^{-3} mol/l Fe^{2+} is indicated by (□).

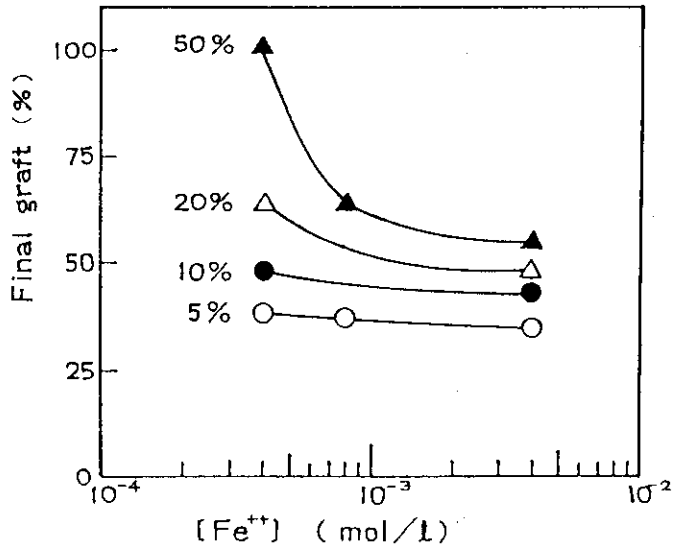

Fig. 2 Final graft percent as a function of Mohr's salt concentration at different monomer concentrations; Concentration of AA (by vol.); (o) 5%, (●) 10%, (△) 20%,(▲) 50%; Preirradiation dose: 5 Mrad; Reaction temperature: 35°C.

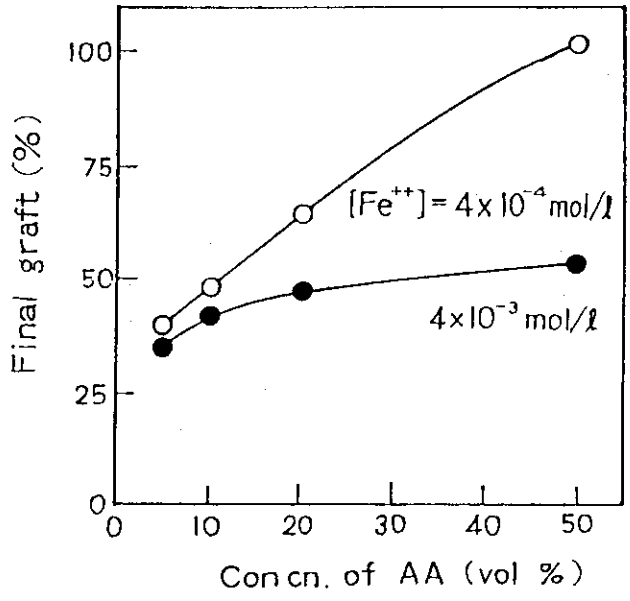

Fig. 3 Final graft percent as a function of monomer concentrations; Preirradiation dose: 5 Mrad; Concentration of Mohr's salt: (o) 4 X 10^{-4} mol/l, (●) 4 X 10^{-3} mol/l; reaction temperature: 35°C.

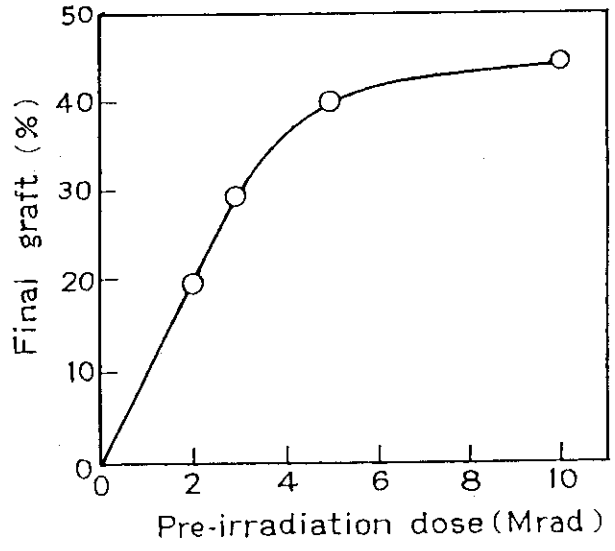

Fig. 4 Final graft percent as a function of preirradiation dose; Concentration of acrylic acid in monomer solution: 5%(by volume); Concentration of Mohr's salt: 4 X 10^{-4} mol/l; Reaction temperature: 35°C.

Table 1 Surface electric resistivity of grafted foam

	Graft (%)	resistivity(ohm)
Starting foam	0.0	10^{16}
Acid	54.8	10^{11}
	91.9	10^{11}
Na-salt	50.4	10^{6}
	105.3	10^{5}

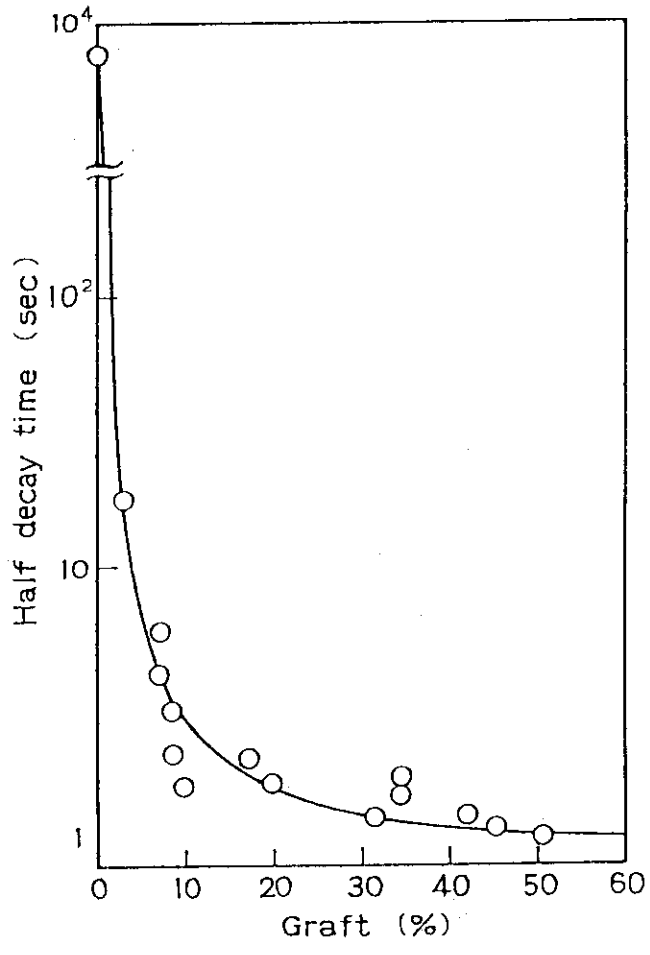

Fig. 5 Half-life of surface potential of grafted foam as a function of graft percent; Relative humidity: 60%.

7. Energy Backscattering of Electron Beams (0.8-1.5MeV) and Absorbed Dose in Thin Films

Dose absorbed in material when electron beams of 0.8-1.5 MeV entered into the material is estimated on the basis of depth-dose distribution curve in the material. However, as the thickness of the target material becomes extremely thinner compared to the range of incident electrons, contribution of backscattering energy from the backing substrate to the dose absorbed in the target becomes important. The contribution of the backscattering energy in the total absorbed dose with 1.0 MeV electrons can be as large as 60% depending on the type of backing material and thickness of the target material.

The number of the backscattering electrons can be calculated using Tabata's empirical formula which relates the number of the backscattering electrons and the incident electron energy on substrates of different materials. The backscattering energy is calculated by multiplying the number of backscattering electrons and their kinetic energy, the latter of which is difficult to obtain experimentally, but can be estimated with the help of computational codes. Two experimental studies, however, are reported on depth-dose curve of two layer structure and of multi-layer structure.

The experimental set up is shown in Fig. 1. A semi-infinitive substrate material such as lead, iron, aluminum, and cellulose triacetate(CTA) was placed 10 cm below the irradiation window of a Van de Graaff. A slab of different numbers of CTA films (1, 3, 5, 10, and 20) was placed on the substrate material and then was irradiated with electrons (1.5 MeV). After the irradiation, the CTA films were subjected to optical density measurement at the wavelength of 280nm to be converted to dose using a calibration line.

An example of the measurements carried out on lead is shown in Fig. 2 where energy dissipation per incident electron is plotted with filled circles as a function of thickness. The plot with open circles

indicates results in a semi-infinite CTA slab for comparison. It is noted from the figure that the dose at the surface of the CTA slab decreased as the number of CTA films increased, and did not decrease when the number of CTA films exceeds 20(0.33 g/cm^2). This result indicates that the backscattering electrons from surface of lead substrate do not reach at the top layer of the CTA film slab.

Similar experiments were carried out on other backing materials and it was found that the increase of the dose on the backing material depends on the atomic number of the backing material. The results are summarized in Fig. 3 in which the energy dissipation in a CTA slab of 20 films on different backing materials is plotted as a function of thickness.

The conclusion derived from the above experimental results is that contribution of backscattering energy from the substrate should be considered for dose measurement of thin layer substance when its thickness becomes extremely smaller compared to the range of incident electrons. (K. Matsuda and T. Kijima)

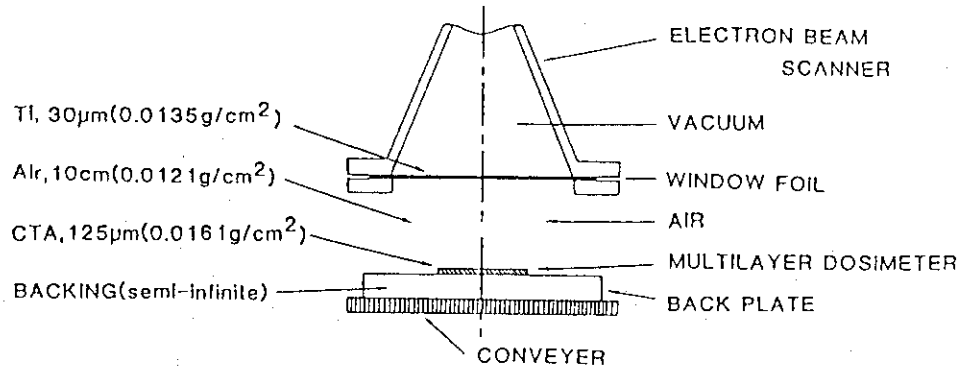

Fig. 1 Experimental set up for energy backscattering measurement of electrons on various semi-infinite backing materials.

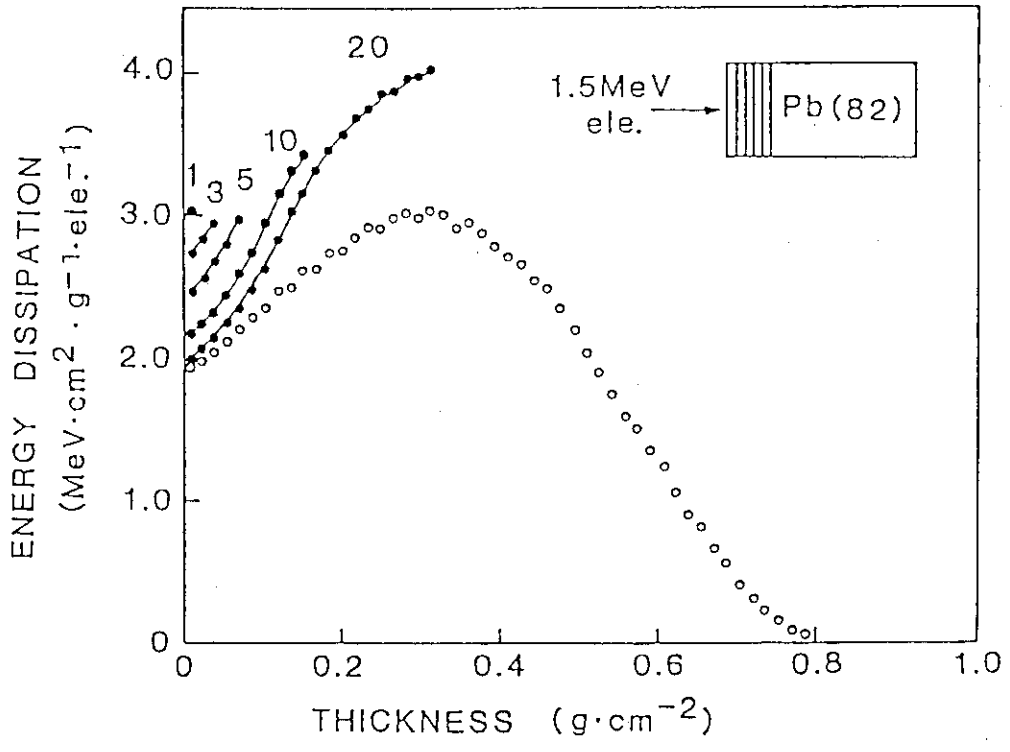

Fig. 2 Comparison of the depth dose profile in a semi-infinite CTA slab (O) with that in various thin CTA slabs (●) backed by a semi-infinite lead slab. Numerals in the figure are the number of CTA films.

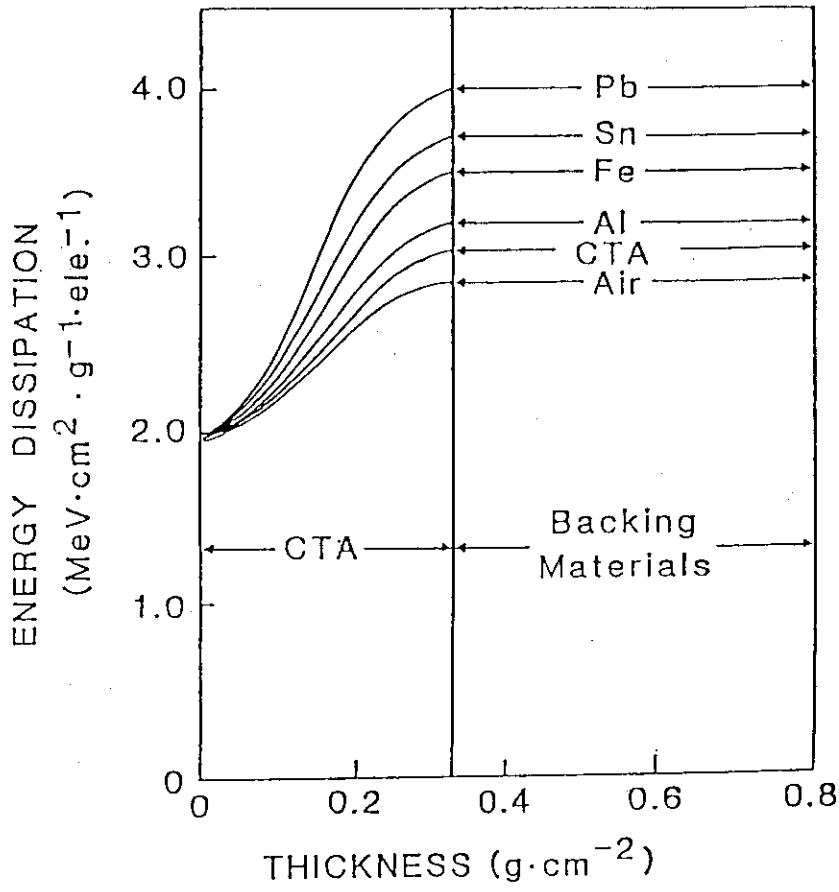

Fig. 3 The depth dose profile in a CTA slab 0.33 g/cm^2 thick with various semi-infinite backing materials at 1.5 MeV electron.

8. Determination of Diffusion Lengths of Electrons in a p-on-n Type GaAs Solar Cell

Knowledge of diffusion lengths of minority carriers and of their change caused by electron irradiation is important to understand the radiation damage of GaAs solar cells in space. Aukerman et al.[1] reported the technique of measuring the diffusion lengths of electrons and holes, the technique consisting of measuring the short circuit current of a GaAs diode during 2 MeV electron irradiation.

We describe the result of measuring the diffusion lengths of electrons, using this technique in a GaAs solar cell which is obtained from Mitsubishi Electric Works. The short circuit current was determined by a digital multimeter (Keithley model 617, equivalent input resistance : 0.1 Ω) which transmits the digitized current data to a microcomputer (Fujitsu, FM8) through a GPIB interface. The solar cell was irradiated with electron beam from a Van de Graaff accelerator (1.0 MeV, 30 μA, spot beam) on a gold plated brass block which was cooled by running water (15 °C) or was heated by a heating wire (150 °C). The short circuit current per unit area of junction, I_{sc} is given by

$$I_{sc} = I_b (dE/dx)\ 1/\eta\ (L_n + L_p + d) \qquad (1)$$

where I_B is an incident electron current density, (dE/dx), energy loss per unit length of the electron path, η , the energy required for producing a pair of electron and holes, and d, width of depletion zone. L_n and L_p are diffusion lengths of electrons in p-region and holes in n-region, respectively. L_p and d are ignored because these values are smaller compared to L_n . Since L_n is related to diffusion constant D_n and life time t_n by eq. (2) and the latter is further related to a number of defects which are proportional to dose, Φ , as shown by eq. (3),

$$L_n = (D_n - t_n) \qquad (2)$$

$$1/t_n = 1/t_{no} + K\Phi \qquad (3)$$

I_{sc} is rewritten as eq. (4) using eq. (1) through (3)

$$I_{sc} = I_B (dE/dx)(1/\eta) \times \frac{L_{n0}}{(1 + Kt_{n0})^{1/2}} \quad (4)$$

The value of (dE/dx) for 1 MeV electrons in eq. (4) can be obtained by the following procedure : (i) the value for (dE/dR) for 1 MeV electrons was calculated to be 1.92 x 10^{-3} MeV·cm^2·mg^{-1} using the empirical range-energy relationship (4b) and range 412 mg·cm^{-2} which was also determined from eq. (4a).

$$R = 412\ E^{(1.265 - 0.0954 \ln E)} \quad (4a)$$

$$(dE/dR) = (E/R)(1.265 - 0.0954 \ln E) \quad (4b)$$

This value was further converted to (dE/dx) multiplying (dE/dR) value by the density of GaAs (5350 mg·cm^{-3}) and was calculated to be 10.3 MeV·cm^{-3}.

In Fig. 1, $(I_{sc}/I_B)^2$ was plotted as a function of dose. Plot(a) was obtained at 15 °C while plot(b) at 150 °C. The plot(b) includes some scattered points due to poor contact during irradiation at 150 °C. The slope, $d(I_B/I_{sc})^2/d\Phi$, is steep in smaller dose region, but this value decreases as dose increases, indicating that the diffusion length becomes smaller as the number of defects which serve as trapping center of electrons increases with dose.

Expanded plots of the low-damage region of the data in Fig. 1 are shown in Fig. 2, where the extrapolation of $(I_B/I_{sc})^2$ values to zero dose gives 4 x 10^{-6} at 15 °C and 2 x 10^{-6} at 150 °C, respectively. The diffusion length at 15 °C was calculated to be 2.2 μm using value of 4.6 eV and 3.1 μm using value of 6.30 eV. The corresponding values at 150 °C were 3.2 μm and 4.3 μm, respectively.

(M. Hatada, K. Matsuda, and S. Hokuyou)

1) L. W. Aukerman, M. F. Miller, and M. McColl, J. Appl. Phys., 38, 685 (1967).

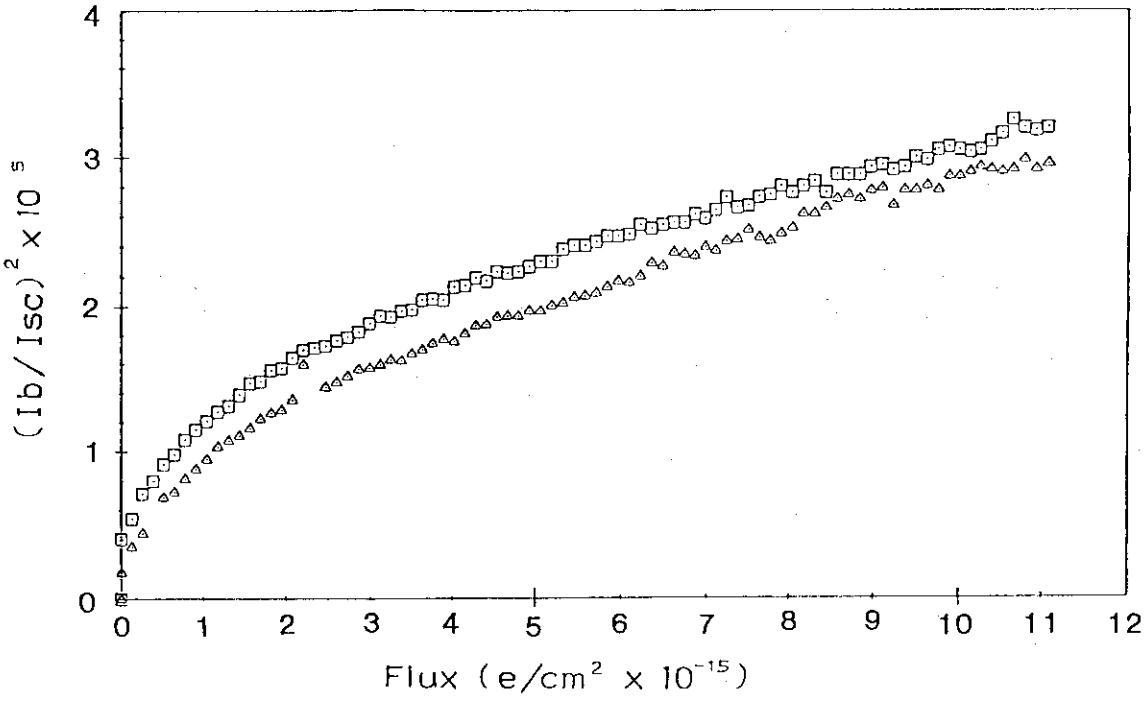

Fig. 1 Variation of the short-circuit/beam current ratio squared with flux for a GaAs solar cell; ⊡ 15°C and △ 150°C.

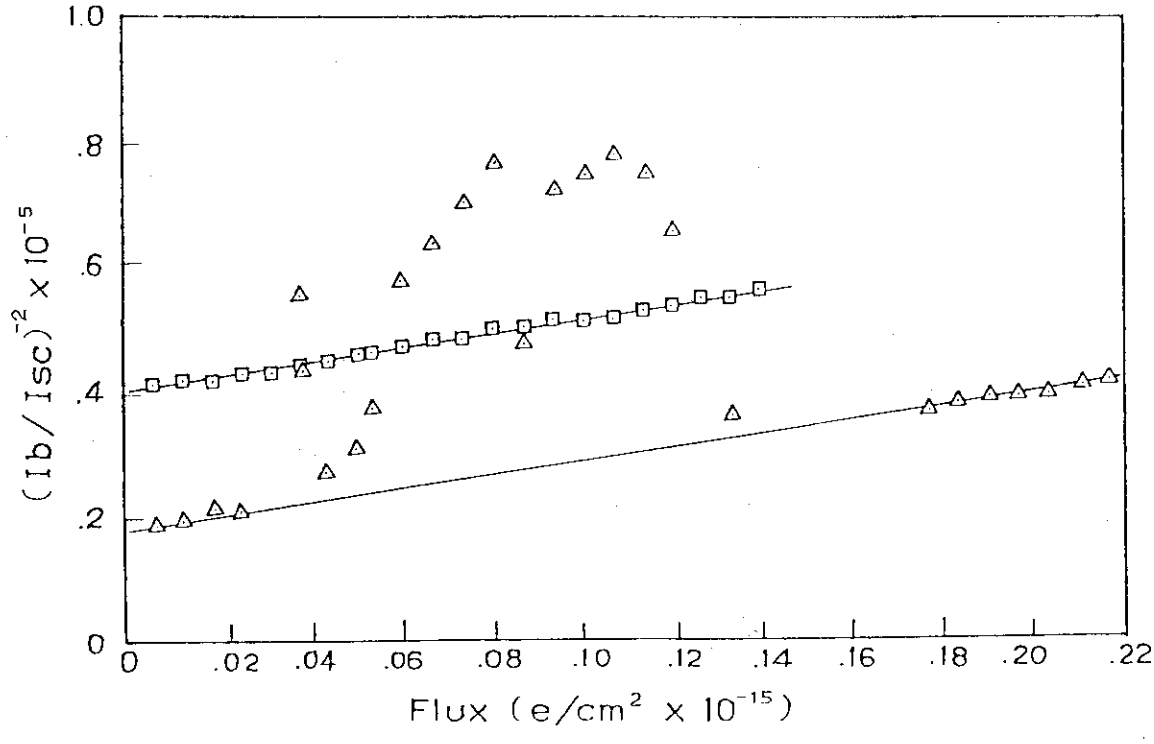

Fig. 2 Expanded plots of the linear low-damage region of the data in Fig. 1 with the multiplication factors of 50 times on the abscissd and of two times on the ordinate; ⊡ 15°C and △ 150°C.

III. LIST OF PUBLICATIONS

1. Published Papers

1....K. Kaji, "Distribution of Poly(Acrylic Acid) in Polyethylene Film", J. Appl. Polym. Sci., 32, 4405(1986).

2....T. Tanaka, C. Inagaki, K. Matsuda, and S. Takaori, "Characteristics of Ethacrynic Acid High Sesnitive Mg^{2+} ATPase in Microsmal Fractions of the Rat Brain", Japanese J. Pharmacol., 42, 351(1986).

*　　*　　*　　*　　*

3....Y. Kanaya and K. Kaji, "Surface Active Polyester Fibers and the Method of Manufacture ", Japanese Patent Application No.61-175378, Jul. 7, 1986.

4....H. Tamura, K. Ogawa,and M. Hatada, "Preparation of Lnagmuir-Blodgett Films from Monomolecular Films", Japanese Patent Application No. 62-015536, Jan. 26, 1987.

5....K. Kaji, M. Hatada, I. Yoshizawa, and C. Kohara,"Preparation of Modified Polyolefine Foam of Open Cell Type", Japanese Patent Application No. 62-057742, Mar. 12, 1987.

2. Oral Presentations

1....T. Okada, T. Asano, J. Takezaki, and M. Hatada, "Electron-Beam Curing of Epoxy Resins", The 52nd Annual Meeting (spring) of the Chemical Society of Japan (Kyoto), Apr. 2, 1986.

2....T. Okada, T. Asano, J. Takezaki, and M. Hatada,"Electron Beam curing of Epoxy Oligomers of Different Molecular Weights", The 32nd Symposium on Polymer Science(Kobe), Jul. 11, 1986.

3....H. Tamura, K. Ogawa, K. Ueda, and M. Hatada,"Polymerization of Langmuir-Blodgett Films of Unsaturated Carboxylic Acids as Studied by FTIR Technique", The Discussion Meeting of the Japanese Society of Applied Physics (Sapporo), Sep. 27, 1986.

4....S. Sugimoto and M. Hatada, "Catalytic Reaction of Iron-Implanted Polyimide Film by Electron-doping", The 39th Discussion Meeint on Colloid and Surface Science (Tsukuba), Oct. 6, 1986.

5....K. Ogawa, H. Tamura, M. Hatada, and T. Ishihara,"Spectroscopic Evaluation and Photo-Reaction Process of Langmuir Films Using Multi-Channel Spectrophotometer", The 3rd International Conference on Langmuir-Blodgett Films, Aug. 27, 1986.

6....K. Ogawa, H. Tamura, K. Ueda, and M. Hatada, "Spectroscopic Evaluation of Langmuir Films(II)", The Discussion Meeting of the Japanese Society of Applied Physics, Mar. 27, 1986.

7....K. Ogawa, H. Tamura, K. Ueda, and M. Hatada, "Spectroscopic Evaluation of Langmuir Films (III)", The Discussion Meeting of the Japanese Society on Applied Physics", Mar. 27, 1986.

IV. EXTERNAL RELATIONS

A training program for scientists and engineers of industries and government organizations was held in the laboratory as one of the courses offered by the Radio-isotope and reactor school, JAERI in Tokyo. This one week program starting Oct. 22 included lectures and laboratory experiments concerned with the radiation chemistry of polymers from its basic subjects to recent application in industries. We welcomed 16 trainees this year.

Some studies in this labaoratory were conducted under the cooperative agreements with Profesors in Kyoto, Osaka and vicinity area:

Prof. Y. Tsuji, Kinki University

Prof. H. Saito, Naruto College of Education

Prof. S. Ohnishi, Kyoto University

Prof. I. Oshiyama, Kyoto University of Industrial Technology

Prof. T. Okada, Ohita University

Prof. K. Hatada, Osaka University

Prof. Y. Ikada, Kyoto University

Three joint research programms have continued this year with industrial companies:

Matsushita Electric Industries, Ltd.

Showa High Polymer Co., Ltd.

Seiren Co., Ltd.

Sanwa Kako Co., Ltd.

A sponsored investigation was made under the contract with the Mitsubishi Electric Corporation.

V. LIST OF SCIENTISTS

[1] Staff Members

Motoyoshi HATADA	Dr., physical chemist, Director
Seizo OKAMURA	Professor emeritus, Kyoto University, Advisor
Yoshiaki NAKASE	Dr., polymer chemist
Siro NAGAI	Dr., physical chemist
Kanako KAJI	Dr., polymer chemist
Shun'ichi SUGIMOTO	Physical chemist
Koji MATSUDA	Physicist
Jun'ichi TAKEZAKI	Physical chemist
Masanobu NISHII	Dr., polymer chemist
Yuuichi SHIMIZU	Physical chemist

[2] Visiting Researcher

Choji KOHARA	Organic chemist, Sanwa Kako Co., Ltd. (May 1986 - Mar. 1987)